ELSEVIER

www.elsevier.nl/locate/jorganchem

Journal of Organometallic Chemistry 613 (2000) 177–199

Journal of Organo metallic Chemistry

Scope and diastereoselectivity of intramolecular [4 + 2] Diels–Alder cycloaddition reactions of (η^6-arene)Ru(DMPP)Cl_2 complexes with dieneophilic ligands

Kent D. Redwine, John H. Nelson *

Department of Chemistry/216, College of Arts and Science, University of Nevada, Reno, NV 89577-0020, USA

Received 28 March 2000; received in revised form 22 May 2000

Abstract

The complexes (η^6-arene)Ru(DMPP)Cl_2 (DMPP = 3,4-dimethyl-1-phenylphosphole; arene = C_6H_6, MeC_6H_5, *p*-$MeC_6H_4CHMe_2$, and C_6Me_6) react with $NaPF_6$ and the dieneophilic ligands: $Ph_2PCH{=}CH_2$ (DPVP), $Me_2NC(O)CH{=}CH_2$ (DMAA), $MeC(O)CH{=}CH_2$ (MVK), $PhSCH{=}CH_2$ (PVS), $PhS(O)CH{=}CH_2$ (PVSO), and 2-vinylpyridine (2VP) to produce [(η^6-arene)Ru(*syn*-*exo*-2-*R*-5,6-dimethyl-7-phenyl-7-phosphabicyclo [2.2.1] hept-5-ene)Cl]PF_6 complexes (R = –PPh_2, –C(O)NMe_2, –C(O)Me, –PhS, –PhS(O), and –2C_5H_4N, respectively) with high diastereo-selectivities. Similar reactions of (η^6-arene)Ru(DMPP)Cl_2 with $NaPF_6$ and allyldiphenyl-phosphine (ADPP) produced the mixed ligand complexes [(η^6-arene)Ru(DMPP) (ADPP)Cl_2]PF_6 which did not undergo subsequent [4 + 2] Diels–Alder cycloadditions even at elevated temperatures. New complexes were characterized by elemental analyses, physical properties, cyclic voltammetry, infrared spectroscopy, ^1H-, $^1H\{^{31}P\}$-, $^{13}C\{^1H\}$-, and $^{31}P\{^1H\}$-NMR spectroscopy and in most cases by X-ray crystallography.

Keywords: Phosphole; [4 + 2] Diels–Alder cycloaddition; Ruthenium; X-ray crystallography

1. Introduction

We have employed the highly efficient and diastereoselective [4 + 2] Diels–Alder *cyclo*-addition reactions of 1H-phospholes [1] and 2H-phospholes [2] with a variety of dieneophiles for the synthesis of a number of conformationally rigid asymmetric chelating ligands. Typical reactions of three-legged piano stool complexes of 3,4-dimethyl-1-phenylphosphole (DMPP) are illustrated in reactions 1–3.

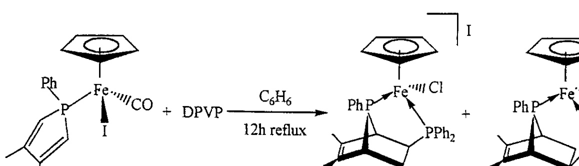

(1) [1c]

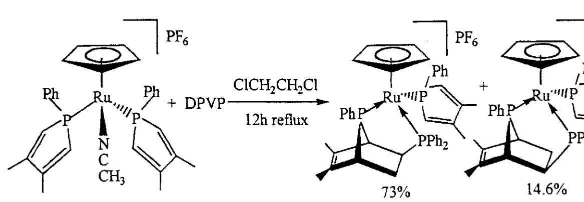

(2) [1d]

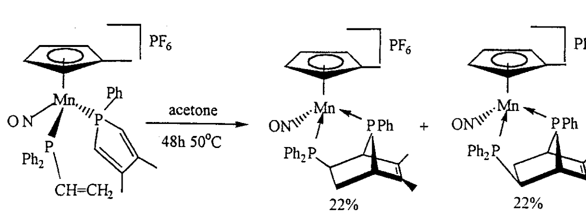

(3) [1f]

Because these reactions occur intramolecularly, within the coordination sphere of a transition metal, of the four possible diastereomers, only the *syn*-*exo* diastereomer of the 2-*R*-5,6-dimethyl- 7-phenyl-7-phosphabicyclo [2.2.1] hept-5-ene is formed [1] (Chart 1).

* Corresponding author. Tel.: + 1-775-7846588; fax: + 1-775-7846804.

E-mail address: jhnelson@equinox.unr.edu (J.H. Nelson).

0022-328X/00/$ - see front matter
PII: S0022-328X(00)00504-0

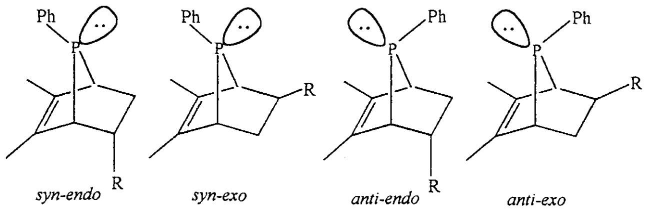

Chart 1.

Recently, organopalladium complexes containing optically pure forms of orthopalladated (1-(dimethylamino)ethyl)naphthalene [3] and (2-(dimethylamino)-ethyl)naphthalene [4] have been used as chiral templates to promote asymmetric modifications of these Diels–Alder cycloaddition reactions with several dieneophilic ligands.

In general these reactions do not occur in the absence of a transition metal. [5] The scope and diastereoselectivity of these transition metal promoted intramolecular [4 + 2] Diels–Alder *cyclo*-additions depends upon the nature of the metal and its ancillary ligands. [1] The diastereo-selectivity is generally thermodynamically controlled and is a primary function of steric effects within the metal's coordination sphere. The $[(\eta^5\text{-}C_5H_5)Ru(DMPP)_{3-n}(\text{dieneophile})_n]PF_6$ system [1d] promotes these reactions with the widest variety of dieneophiles yet found and in some cases with quite high diastereoselectivity.

Ruthenium(II) complexes of the type $[(\eta^6\text{-arene})Ru(AB)X]^+X^-$, where AB is an optically pure bidentate ligand and X is a halide, are efficient catalysts for the asymmetric transfer hydro-genation of ketones [6], alkenes [7], and imines [8]. The potential catalytic activity of new species of this type containing conformationally rigid asymmetric bidentate ligands, together with our desire to gain further insight regarding those factors that determine the scope and diastereoselectivity of the metal promoted intramolecular [4 + 2] Diels–Alder cycloaddition reactions of phospholes prompted us to investigate the reactions of the $(\eta^6\text{-arene})Ru(DMPP)Cl_2$ complexes with selected dieneophilic ligands.

2. Experimental

2.1. Reagents and physical measurements

All chemicals were reagent grade and were used as received from commercial sources (Aldrich, Fischer, Organometallics, Alpha/AESAR) or synthesized as described below. DMPP [9] and the $(\eta^6\text{-arene})Ru(R_3P)Cl_2$ [10] complexes were synthesized by literature methods. Solvents were dried by standard procedures and stored over Linde type 4 Å molecular sieves. All reactions involving phosphines were conducted under a purified nitrogen atmosphere by standard Schlenk techniques. Elemental analyses were performed by Galbraith Laboratories, Knoxville, TN. Melting points were determined on a Mel-Temp apparatus and are uncorrected. NMR spectra were recorded on acetone-d_6 or nitromethane-d_3 solutions with a Varian Unity Plus-500 FT spectrometer operating at 500 MHz for ^1H, 202 MHz for ^{31}P, and 125 MHz for ^{13}C. Proton and carbon chemical shifts were referenced to residual solvent resonances and phosphorus chemical shifts were referenced to an external 85% aqueous solution of H_3PO_4. All shifts to low field, high frequency are positive. FT-IR spectra were recorded as Nujol mulls on CsI windows on a Perkin–Elmer BX spectrometer. Cyclic voltammograms were recorded at 25°C in freshly distilled CH_2Cl_2 containing 0.1 M tetra-butylammonium hexafluorophosphate using a BAS CV50-W voltammetric analyzer. A three electrode system was used. The working electrode was a platinum disk, the auxiliary electrode was a platinum wire, and the reference electrode was Ag–AgCl (aqueous) separated from the cell by a Luggin capillary. The F_c/F_c^+ couple occured at 480 mV under the same conditions.

2.2. Synthesis

All of the $[(\eta^6\text{-arene})Ru(DMPP)(\text{dieneophile})Cl]PF_6$ complexes were prepared in the following manner. To a solution containing 1.0 mmol of the appropriate $(\eta^6\text{-arene})Ru$ $(DMPP)Cl_2$ complex in 25 ml of CH_2Cl_2 was added 1.0 mmol of solid $NaPF_6$. The reaction vessel was purged with nitrogen for 30 min. Then 1.1 mmol of the appropriate dieneophilic ligand was added via syringe and the reaction mixture was stirred under nitrogen at ambient temperature for 48 h. The initially deep red solution became orange or yellow, depending upon the ligand, as the reaction proceeded. The solution was gravity filtered to remove NaCl and the filtrate was taken to dryness on a rotary evaporator. The resulting solid or oil was dissolved in a minimum amount of CH_2Cl_2, and after filtering the solution, ether was added to the filtrate to induce crystallization. The yellow or orange microcrystals that resulted were isolated by filtration, washed with ether, and dried under vacuum at ambient temperature. The yields, colors, melting points, and analytical data are given in Table 1. $^{31}P\{^1H\}$-NMR and IR data are given in Table 2 and ^1H- and $^{13}C\{^1H\}$-NMR data follow.

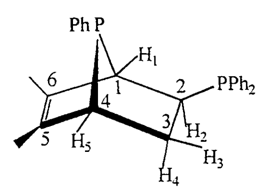

2.2.1. $[(\eta^6\text{-}C_6Me_6)Ru(DMPP)(DPVP)Cl]PF_6$ (**1**)

^1H-NMR (499.8 MHz, CD_3NO_2, 25°C) δ 8.0–7.3 (m, 15H, Ph), 3.97 (dd, $^3J(H_1H_2) = 3.0$ Hz, $^4J(H_1H_5) = 2.0$ Hz, 1H, H_1), 3.33 (ddddd, $^3J(PH) = 41.0$ Hz, $^3J(H_2H_4) = 9.0$ Hz, $^2J(PH) = 6.5$ Hz, $^3J(H_1H_2) = 3.0$ Hz, $^3J(H_2H_3) = 0.5$ Hz, 1H, H_2), 3.06 (dd, $^3J(H_3H_5) = 4.0$ Hz,

Table 1
Percent yields, colors, melting points, and analytical data for compounds **1**–**20**

Arene	Dieneophile	%yield	Color	m.p. (°C)	%C (Calc.)	%C (Found)	%H (Calc.)	%H (Found)	%Cl (Calc.)	%Cl (Found)
(**1**) C_6Me_6	DPVP	58.5	Yellow	250–251	54.01	54.06	5.21	5.14	4.19	4.10
(**2**) C_6Me_6	PVS	54.6	Orange	240–241	50.05	49.86	5.08	5.12	4.62	4.39
(**3a**) C_6Me_6	PVSO	72.0	Orange	265–267	49.03	48.94	4.98	4.73	4.52	4.37
(**3b**) C_6Me_6	PVSO	72.0	Yellow	265–267	49.03	48.87	4.98	4.85	4.52	4.46
(**4**) C_6Me_6	MVK	62.3	Red	294–296	47.92	47.79	5.27	5.16	5.05	4.93
(**5**) C_6Me_6	DMAA	71.4	Red	280–281	47.66	47.58	5.47	5.39	4.85	4.68
(**6**) C_6Me_6	2VP	56.0	Orange	227–228	50.53	50.41	5.16	5.02	4.81	4.63
(**7**) *p*-$MeC_6H_4CHMe_2$	DPVP	57.0	Yellow	243–245	48.58	48.39	4.99	4.82	4.78	4.64
(**8**) *p*-$MeC_6H_4CHMe_2$	PVS	58.7	Orange	221–222	48.70	48.56	4.73	4.61	4.79	4.58
(**9**) *p*-$MeC_6H_4CHMe_2$	PVSO	68.2	Yellow	169–171	47.67	47.60	4.63	4.58	4.69	4.61
(**10**) *p*-$MeC_6H_4CHMe_2$	MVK	42.7	Red	126–127	46.35	46.27	4.90	4.69	5.26	5.12
(**11**) *p*-$MeC_6H_4CHMe_2$	DMAA	59.0	Red	210–211	46.08	45.93	5.26	5.18	5.04	4.86
(**12**) *p*-$MeC_6H_4CHMe_2$	2VP	53.3	Yellow	135–136	49.14	48.75	4.80	4.67	5.00	4.83
(**13**) C_6H_6	DPVP	50.0	Yellow	210–212	50.59	50.38	4.21	4.14	4.67	4.51
(**14**) C_6H_6	PVS	57.6	Orange	217–218	45.67	45.52	3.95	3.86	5.18	5.09
(**15**) C_6H_6	2VP	76.3	Yellow	265–266	46.00	45.84	3.98	3.87	5.43	5.25
(**16**) MeC_6H_5	DPVP	60.5	Yellow	270–272	51.22	51.09	4.39	4.50	4.58	4.62
(**17**) MeC_6H_5	PVS	41.0	Yellow	170–172	49.05	48.75	4.16	4.02	5.08	4.94
(**18**) MeC_6H_5	2VP	68.3	Orange	268–270	46.84	46.76	4.20	4.09	5.32	5.17
(**19**) C_6Me_6	ADPP	65.4	Red	291–293	56.65	56.39	5.56	5.47	4.29	4.18
(**20**) *p*-$MeC_6H_4CHMe_2$	ADPP	70.1	Orange	284–286	53.49	53.39	5.06	4.98	4.27	4.13

$^4J(H_1H_5) = 2.0$ Hz, 1H, H_5), 2.27 (dddd, $^2J(PH) = 23.5$ Hz, $^2J(H_3H_4) = 13.5$ Hz, $^2J(H_3H_5) = 4.0$ Hz, $^3J(H_2H_3) = 0.5$ Hz, 1H, H_3), 1.83 (s, 3H, CH_3), 1.71 (s, 18H, η^6-C_6Me_6), 1.53 (dddd, $^3J(PH) = 23.5$ Hz, $^3J(PH) = 20.0$ Hz, $^2J(H_3H_4) = 13.5$ Hz, $^3J(H_2H_4) = 9.0$ Hz, 1H, H_4), 1.36 (s, 3H, CH_3). $^{13}C\{^1H\}$-NMR (125.7 MHz, CD_3NO_2, 25°C) δ 140.20 (dd, $^2J(PC) = 2.6$ Hz, $^4J(PC) = 1.9$ Hz, C_5), 134.05 (dd, $^1J(PC) = 41.6$ Hz, $^3J(PC) = 0.6$ Hz, C_i), 132.72 (d, $^2J(PC) = 7.5$ Hz, C_o), 132.64 (d, $^2J(PC) = 12.4$ Hz, C_o), 131.49 (d, $^4J(PC) = 3.5$ Hz, C_p), 131.24 (d, $^4J(PC) = 2.5$ Hz, C_p), 131.18 (d, $^2J(PC) = 12.6$ Hz, C_o), 131.15 (d, $^4J(PC) = 2.5$ Hz, C_o), 130.72 (dd, $^2J(PC) = 15.3$ Hz, $^3J(PC) = 0.8$ Hz, C_6), 129.59 (d, $^1J(PC) = 50.9$ Hz, C_i), 129.14 (d, $^3J(PC) = 10.8$ Hz, C_m), 129.01 (d, $^3J(PC) = 9.4$ Hz, C_m), 128.73 (dd, $^1J(PC) = 38.3$ Hz, $^3J(PC) = 1.6$ Hz, C_i), 128.49 (d, $^3J(PC) = 8.2$ Hz, C_m), 106.34 (apparent t, $^2J(PC) = {^2J(P'C)} = 2.1$ Hz, η^6-C_6Me_6), 58.05 (dd, $^1J(PC) = 34.1$ Hz, $^3J(PC) = 12.7$ Hz, C_1), 50.12 (dd, $^1J(PC) = 35.5$ Hz, $^2J(PC) = 0.6$ Hz, C_4), 34.27 (dd, $^1J(PC) = 40.0$ Hz, $^2J(PC) = 29.0$ Hz, C_2), 31.17 (dd, $^2J(PC) = 10.2$ Hz, $^2J(PC) = 1.5$ Hz, C_3), 14.66 (s, η^6-C_6Me_6), 13.97 (apparent t, $^3J(PC) = {^4J(PC)} = 1.8$ Hz, CH_3), 12.24 (d, $^3J(PC) = 3.3$ Hz, CH_3).

2.2.2. *[(η^6-C_6Me_6)Ru(DMPP)(PVS)Cl]PF_6* (**2**)

^1H-NMR (499.8 MHz, CD_3NO_2, 25°C) δ 7.92 (m, 2H, H_o, PPh), 7.59 (m, 1H, H_p, PPh), 7.46 (m, 7H, H_m, PPh, $H_{o,m,p}$, SPh), 4.04 (apparent ddt, $^3J(PH) = 37.0$ Hz, $^3J(H_2H_4) = 9.5$ Hz, $^3J(H_2H_3) = {^3J(H_1H_2)} = 2.0$ Hz, 1H, H_2), 3.75 (dd, $^3J(H_3H_5) = 3.0$ Hz, $^4J(H_1H_5) = 2.0$ Hz, 1H, H_5), 3.48 (apparent q, $^2J(PH) = {^3J(H_1H_2)} = {^4J(H_2H_5)} = 2.0$ Hz, 1H, H_2), 2.31 (ddd, $^3J(PH) = 25.0$ Hz, $^2J(H_3H_4) = 14.5$ Hz, $^3J(H_2H_4) = 9.5$ Hz, 1H, H_4), 2.11 (s, 18H, η^6-C_6Me_6), 1.80 (apparent quin, $^4J(PH) = {^5J(HH)} = 1.0$ Hz, 3H, CH_3), 1.68 (ddd, $^2J(H_3H_4) = 14.5$ Hz, $^3J(H_3H_5) = 3.0$ Hz, $^3J(H_2H_3) = 2.0$ Hz, 1H, H_3), 1.56 (q, $^5J(HH) = 1.0$ Hz, 3H, CH_3). $^{13}C\{^1H\}$-NMR (125.7 MHz, CD_3NO_2, 25°C) δ 140.60 (s, C_i, SPh), 133.52 (d, $^2J(PC) = 7.5$ Hz, C_o, PPh), 131.74 (d, $^4J(PC) = 2.3$ Hz, C_p, PPh), 130.48 (s, C_5), 129.61 (s, C_6), 129.10 (s, C_m, SPh), 128.80 (s, C_o, SPh), 128.71 (s, C_p, SPh), 128.31 (d, $^3J(PC) = 9.7$ Hz, C_m, PPh), 126.53 (d, $^1J(PC) = 41.0$ Hz, C_i, PPh), 101.20 (d, $J(PC) = 2.0$ Hz, η^6-C_6Me_6), 57.68 (d, $^1J(PC) = 38.1$ Hz, C_1), 45.43 (d, $^1J(PC) = 28.3$ Hz, C_4), 42.36 (d, $^2J(PC) = 32.2$ Hz, C_2), 32.54 (d, $^2J(PC) = 20.1$ Hz, C_3), 14.99 (s, C_6Me_6), 13.41 (d, $^3J(PC) = 2.6$ Hz, CH_3), 12.98 (d, $^3J(PC) = 2.3$ Hz, CH_3).

Table 2
$^{31}P\{^1H\}$-NMR and infrared data for complexes **1**–**20** [a]

Compound	δ P_7 (ppm)	δ P_2 (ppm)	$^2J(PP)$ (Hz)	δ PF_6^- (ppm)	$^1J(PF)$ (Hz)	%DE	ν(CO or SO) (cm^{-1})	ν(PF) (cm^{-1})
1a	148.06	63.93	54.9	−145.07	707	82		837, 556
1b	142.65	58.96	55.9	−145.07	707			
2a	147.64			−145.00	708	55.6		831, 557
2b	145.10			−145.00	708			
3a	146.95			−145.00	708	50	1096	832, 557
3b	147.29			−145.00	708			
4	117.75			−145.00	708	>99	1699	836, 557
5	119.13			−145.00	708	>99	1699	845, 557
6	122.21			−145.00	708	>99	840, 557	
7a	142.72	59.00	56.1	−145.00	707	87.8	837, 556	
7b	139.23	45.17	50.2	−145.00	707			
8a	146.17			−145.00	708	44.9	829, 556	
8b	146.25			−145.00	708			
9	143.74			−145.00	708	>99	1078	831, 557
10	114.18			−145.00	708	>99	1700	838, 556
11	116.09			−145.00	708	>99	1699	845, 557
12	119.73			−144.99	708	>99	834, 558	
13	141.99	59.51	57.7	−145.10	708	>99	836, 558	
14a	144.33			−145.12	708	84.2	843, 558	
14b	140.69			−145.12	708			
15	118.40			−145.00	708	>99	843, 557	
16a	142.75	56.50	57.3	−145.04	708	86	835, 557	
16b	138.49	47.29	51.6	−145.04	708			
17a	145.22			−144.99	708	85.8	837, 557	
17b	141.58			−144.99	708			
18	119.60			−145.00	707	>99	833, 556	
19	29.44	29.09	56.7	−144.90	713		843, 556	
20	28.47	25.16	53.4	−145.00	708		835, 556	

[a] Compounds numbered **a** are the major diastereomer while those numbered **b** are the minor diastereomer.

*2.2.3. [(η⁶-C₆Me₆)Ru(DMPP)(PVSO)Cl]PF₆ (**3a**,**b**)*

^{1}H-NMR (499.8 MHz, CD_3NO_2, 25°C) (**3a**) δ 8.25 (m, 2H, H_o, SPh), 7.58–7.88 (m, 8H, $H_{m,p}$, SPh, $H_{o,m,p}$, PPh), 4.07 (dddd, ^3J(PH) = 37.5 Hz, $^3J(H_2H_4)$ = 8.5 Hz, $^3J(H_1H_2)$ = 2.5 Hz, $^3J(H_2H_3)$ = 1.0 Hz, 1H, H_2), 3.95 (apparent t, $^3J(H_1H_2)$ = $^4J(H_1H_5)$ = 2.5 Hz, 1H, H_1), 3.10 (dd, $^4J(H_1H_5)$ = 2.5 Hz, $^3J(H_3H_5)$ = 2.0 Hz, 1H, H_5), 2.11 (ddd, $^2J(H_3H_4)$ = 14.0 Hz, $^3J(H_3H_5)$ = 2.0 Hz, $^3J(H_2H_3)$ = 1.0 Hz, 1H, H_3), 1.95 (s, 18H, η^6-C_6Me_6), 1.86 (s, 3H, CH_3), 1.40 (ddd, ^3J(PH) = 21.5 Hz, $^2J(H_3H_4)$ = 14.0 Hz, $^3J(H_2H_4)$ = 8.5 Hz, 1H, H_4), 1.38 (s, 3H, CH_3). (**3b**) δ 7.90 (m, 2H, H_o, PPh), 7.76 (m, 2H, H_o, SPh), 7.68 (m, 1H, H_p, SPh), 7.67 (m, 2H, H_m, SPh), 7.64 (m, 1H, H_p, PPh), 7.53 (m, 2H, H_m, PPh), 4.50 (dddd, ^3J(PH) = 40.0 Hz, $^3J(H_2H_4)$ = 8.8 Hz, $^3J(H_1H_2)$ = 2.0 Hz, $^3J(H_2H_3)$ = 1.5 Hz, 1H, H_2), 3.84 (apparent dq, $^3J(H_3H_5)$ = 4.0 Hz, ^2J(PH) = $^3J(H_4H_5)$ = $^4J(H_1H_5)$ = 2.0 Hz, 1H, H_5), 3.26 (apparent q, ^2J(PH) = $^3J(H_1H_2)$ = $^4J(H_1H_5)$ = 2.0 Hz, 1H, H_1), 2.76 (ddd, $^2J(H_3H_4)$ = 15.0 Hz, $^3J(H_3H_5)$ = 4.0 Hz, $^3J(H_2H_3)$ = 1.5 Hz, 1H, H_3), 2.29 (dddd, ^3J(PH) = 25.0 Hz, $^2J(H_3H_4)$ = 15.0 Hz, $^3J(H_2H_4)$ = 8.8 Hz, $^3J(H_4H_5)$ = 2.0 Hz, 1H, H_4), 2.13 (s, 18H, η^6-C_6Me_6), 1.86 (s, 3H, CH_3), 1.59 (s, 3H, CH_3). $^{13}C\{^1H\}$-NMR (125.7 MHz, CD_3NO_2, 25°C) (**3a**) δ 140.76 (s, C_5), 140.64 (s, C_6), 133.88 (s, C_p, SPh), 132.98 (broad d, ^2J(PC) = 14.7 Hz, C_o, PPh), 132.28 (broad s, C_o, PPh), 132.05 (d, ^4J(PC) = 2.6 Hz, C_p, PPh), 129.49 (s, C_m, SPh), 129.38 (broad s, C_m, PPh), 128.83 (broad d, ^3J(PC) = 6.2 Hz, C_m, PPh), 127.85 (s, C_o, SPh), 125.20 (d, ^1J(PC) = 41.6 Hz, C_i, PPh), 108.17 (d, J(PC) = 2.0 Hz, η^6-C_6Me_6), 65.28 (d, ^2J(PC) = 34.8 Hz, C_2), 52.07 (d, ^1J(PC) = 31.9 Hz, C_1), 48.51 (d, ^1J(PC) = 34.3 Hz, C_4), 28.31 (d, ^2J(PC) = 10.6 Hz, C_3), 15.22 (s, η^6-C_6Me_6), 13.93 (d, ^3J(PC) = 1.8 Hz, CH_3), 12.63 (d, ^3J(PC) = 3.1 Hz, CH_3). (**3b**) δ 141.57 (s, C_5), 139.44 (s, C_6), 133.63 (d, ^2J(PC) = 7.8 Hz, C_o, PPh), 132.49 (s, C_p, SPh), 132.38 (d, ^4J(PC) = 2.4 Hz, C_p, PPh), 129.05 (s, C_m, SPh), 128.69 (d, ^3J(PC) = 9.9 Hz, C_m, PPh), 127.92 (s, C_i, SPh), 126.03 (s, C_o, SPh), 124.93 (d, ^1J(PC) = 42.6 Hz, C_i, PPh), 106.45 (d, J(PC) = 1.9 Hz, η^6-C_6Me_6), 60.87 (d, ^2J(PC) = 33.7 Hz, C_2), 53.79 (d, ^1J(PC) = 35.3 Hz, C_1), 44.74 (d, ^1J(PC) = 30.3 Hz, C_4), 27.80 (d, ^2J(PC) = 18.7 Hz, C_3), 15.07 (s, η^6-C_6Me_6), 13.57 (d, ^3J(PC) = 2.8 Hz, CH_3), 12.78 (d, ^3J(PC) = 2.8 Hz, CH_3).

*2.2.4. [(η⁶-C₆Me₆)Ru(DMPP)(MVK)Cl]PF₆ (**4**)*

^{1}H-NMR (499.8 MHz, CD_3NO_2, 25°C) δ 7.90 (m, 2H, H_o), 7.54 (m, 1H, H_p), 7.46 (m, 2H, H_m), 4.06 (apparent quin, ^2J(PH) = $^3J(H_3H_5)$ = $^3J(H_4H_5)$ = $^4J(H_1H_5)$ = 2.0 Hz, 1H, H_5), 3.40 (dddd, ^3J(PH) = 22.5 Hz, $^3J(H_2H_4)$ = 10.0 Hz, $^3J(H_2H_3)$ = 4.5 Hz, $^3J(H_1H_2)$ = 2.0 Hz, 1H, H_2), 3.14 (apparent q, ^2J(PH) = $^3J(H_1H_2)$ = $^4J(H_1H_5)$ = 2.0 Hz, 1H, H_1), 2.68 (s, 3H, $CH_3C(O)$), 2.19 (m, 1H, H_4), 2.02 (m, 1H, H_3), 1.97 (s, 18H, η^6-C_6Me_6), 1.85 (s, 3H, CH_3), 1.46 (s, 3H, CH_3). $^{13}C\{^1H\}$-NMR (125.7 MHz, CD_3NO_2, 25°C) δ 231.82 (s, C=O), 138.89 (s, C_5), 134.67 (d, ^3J(PC) = 2.0 Hz, C_6), 133.25 (d, ^2J(PC) = 7.9 Hz, C_o), 131.29 (d, ^4J(PC) = 2.5 Hz, C_p), 128.15 (d, ^3J(PC) = 9.7 Hz, C_m), 127.53 (d, ^1J(PC) = 42.4 Hz, C_i), 97.86 (d, J(PC) = 2.5 Hz, η^6-C_6Me_6), 49.35 (d, ^2J(PC) = 15.7 Hz, C_2), 49.22 (d, ^1J(PC) = 30.9 Hz, C_1), 47.41 (d, ^1J(PC) = 29.4 Hz, C_4), 34.25 (s, $CH_3C(O)$), 30.54 (d, ^2J(PC) = 24.1 Hz, C_3), 14.81 (s, η^6-C_6Me_6), 13.14 (d, ^3J(PC) = 2.3 Hz, CH_3), 12.54 (d, ^3J(PC) = 2.3 Hz, CH_3).

*2.2.5. [(η⁶-C₆Me₆)Ru(DMPP)(DMAA)Cl]PF₆ (**5**)*

^{1}H-NMR (499.8 MHz, CD_3NO_2, 25°C) δ 7.89 (m, 2H, H_o), 7.53 (m, 1H, H_p), 7.47 (m, 2H, H_m), 3.92 (apparent dt, $^3J(H_3H_5)$ = 4.0 Hz, $^4J(H_1H_5)$ = ^2J(PH) = 2.0 Hz, 1H, H_5), 3.27 (dddd, ^3J(PH) = 22.0 Hz, $^3J(H_2H_4)$ = 9.0 Hz, $^3J(H_2H_3)$ = 5.0 Hz, $^3J(H_1H_2)$ = 1.5 Hz, 1H, H_2), 3.23 (s, 3H, NCH_3), 3.19 (apparent td, ^2J(PH) = $^3J(H_1H_5)$ = 2.0 Hz, $^3J(H_1H_2)$ = 1.5 Hz, 1H, H_1), 3.14 (s, 3H, NCH_3), 2.03 (m, 1H, H_3), 1.95 (m, 1H, H_4), 1.93 (s, 18H, η^6-C_6Me_6), 1.86 (s, 3H, CH_3), 1.46 (s, 3H, CH_3). $^{13}C\{^1H\}$-NMR (125.7 MHz, CD_3NO_2, 25°C) δ 181.42 (s, C=O), 139.11 (s, C_5), 135.49 (d, ^2J(PC) = 1.6 Hz, C_6), 133.17 (d, ^2J(PC) = 8.2 Hz, C_o), 131.03 (d, ^4J(PC) = 2.0 Hz, C_p), 128.28 (d, ^1J(PC) = 40.1 Hz, C_i), 128.13 (d, ^3J(PC) = 9.3 Hz, C_m), 98.89 (d, J(PC) = 2.4 Hz, η^6-C_6Me_6), 53.30 (d, ^1J(PC) = 31.6 Hz, C_1), 46.45 (d, ^1J(PC) = 28.4 Hz, C_4), 39.78 (d, ^2J(PC) = 15.7 Hz, C_2), 38.67 (s, NCH_3), 37.74 (s, NCH_3), 29.29 (d, ^2J(PC) = 23.9 Hz, C_3), 14.59 (s, η^6-C_6Me_6), 13.14 (d, ^3J(PC) = 2.4 Hz, CH_3), 12.56 (s, ^3J(PC) = 2.4 Hz, CH_3).

*2.2.6. [(η⁶-C₆Me₆)Ru(DMPP)(2VP)Cl]PF₆ (**6**)*

^{1}H-NMR (499.8 MHz, CD_3NO_2, 25°C) δ 8.92 (dd, $^3J(H_aH_b)$ = 6.0 Hz, $^4J(H_aH_c)$ = 1.5 Hz, 1H, H_a), 8.00 (m, 2H, H_o), 7.89 (apparent td, $^3J(H_bH_c)$ = $^3J(H_cH_d)$ = 8.0 Hz, $^4J(H_aH_c)$ = 1.5 Hz, 1H, H_c),

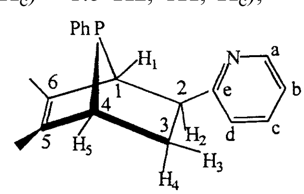

7.54 (m, 1H, H_p), 7.46 (m, 2H, H_m), 7.41 (ddd, $^3J(H_bH_c)$ = 8.0 Hz, $^3J(H_aH_b)$ = 6.0 Hz, $^4J(H_bH_d)$ = 1.5 Hz, 1H, H_b), 7.37 (dd, $^3J(H_cH_d)$ = 8.0 Hz, $^4J(H_bH_d)$ = 1.5 Hz, 1H, H_d), 4.00 (apparent quin, ^2J(PH) = $^4J(H_1H_5)$ = $^3J(H_3H_5)$ = $^3J(H_4H_5)$ = 1.5 Hz, 1H, H_5), 3.43 (dddd, ^3J(PH) = 24.5 Hz, $^3J(H_2H_4)$ = 10.5 Hz, $^3J(H_2H_3)$ = 5.0 Hz, $^3J(H_1H_2)$ = 1.5 Hz, 1H, H_2), 2.65 (apparent q, ^2J(PH) = $^4J(H_1H_5)$ = $^3J(H_1H_2)$ = 1.5 Hz, 1H, H_1), 2.36 (dddd, ^3J(PH) = 33.0 Hz, $^2J(H_3H_4)$ = 12.5 Hz, $^3J(H_2H_4)$ = 10.5 Hz, $^3J(H_4H_5)$ = 1.5 Hz, 1H,

H_4), 2.24 (dddd, $^2J(H_3H_4) = 12.5$ Hz, $^3J(H_2H_3) = 5.0$ Hz, $^3J(H_3H_5) = 1.5$ Hz, 1H, H_3), 1.95 (s, 18H, η^6-C_6Me_6), 1.88 (s, 3H, CH_3), 1.45 (s, 3H, CH_3). $^{13}C\{^1H\}$-NMR (125.7 MHz, CD_3NO_2, 25°C) δ 167.62 (s, C_a), 159.71 (d, $^3J(PC) = 6.7$ Hz, C_e), 138.93 (s, C_c), 136.66 (s, C_5), 135.03 (s, C_6), 133.84 (d, $^2J(PC) = 7.5$ Hz, C_o), 131.01 (d, $^4J(PC) = 2.2$ Hz, C_p), 128.45 (d, $^1J(PC) = 42.0$ Hz, C_i), 127.76 (d, $^3J(PC) = 9.3$ Hz, C_m), 127.34 (s, C_d), 123.99 (s, C_b), 100.68 (d, $J(PC) = 2.3$ Hz, η^6-C_6Me_6), 49.07 (d, $^1J(PC) = 30.2$ Hz, C_1), 47.18 (d, $^1J(PC) = 32.3$ Hz, C_4), 46.82 (d, $^2J(PC) = 17.7$ Hz, C_2), 31.18 (d, $^2J(PC) = 25.9$ Hz, C_3), 14.95 (s, η^6-C_6Me_6), 13.10 (d, $^3J(PC) = 2.8$ Hz, CH_3), 12.55 (d, $^3J(PC) = 2.4$ Hz, CH_3).

2.2.7. *[(η⁶-p-MeC₆H₄CHMe₂)Ru(DMPP)(DPVP)-Cl]PF₆ (**7**)*

^{1}H-NMR (499.8 MHz, CD_3NO_2, 25°C) δ 8.0–7.5 (m, 15H, Ph), 5.91 (dd, $^3J(HH) = 6.0$ Hz, $J(PH) = 1.0$ Hz, 1H. Cy), 5.62 (d, $^3J(HH) = 6.0$ Hz, 1H, Cy), 5.45 (d, $^3J(HH) = 6.0$ Hz, 1H, Cy), 5.22 (d, $^3J(HH) = 6.0$ Hz, 1H, Cy), 3.87 (apparent q, $^4J(H_1H_5) = {}^2J(PH) = {}^3J(H_1H_2) = 2.0$ Hz, 1H, H_1), 3.56 (ddddd, $^3J(PH) = 41.5$ Hz, $^3J(H_2H_4) = 9.5$ Hz, $^2J(PH) = 5.5$ Hz, $^3J(H_1H_2) = 2.0$ Hz, $^3J(H_2H_3) = 0.5$ Hz, 1H, H_2), 3.19 (dd, $^3J(H_3H_5) = 4.0$ Hz, $^4J(H_1H_5) = 2.0$ Hz, 1H, H_5), 2.40 (dddd, $^2J(PH) = 23.5$ Hz, $^2J(H_3H_4) = 13.0$ Hz, $^3J(H_3H_5) = 4.0$ Hz, $^3J(H_2H_3) = 0.5$ Hz, 1H, H_3), 2.10 (sept, $^3J(HH) = 7.0$ Hz, 1H, CH), 1.94 (s, 3H, CH_3), 1.70 (s, 3H, CH_3). 1.67 (dddd, $^3J(PH) = 22.5$ Hz, $^3J(PH) = 19.5$ Hz, $^2J(H_3H_4) = 13.0$ Hz, $^3J(H_2H_4) = 9.5$ Hz, 1H, H_4), 1.49 (s, 3H, CH_3), 1.10 (d, $^3J(HH) = 7.0$ Hz, 3H, CH_3), 0.94 (d, $^3J(HH) = 7.0$ Hz, CH_3). $^{13}C\{^1H\}$-NMR (125.7 MHz, CD_3NO_2, 25°C) δ 139.05 (dd, $^2J(PC) = 2.5$ Hz, $^3J(PC) = 1.0$ Hz, C_5), 134.81 (d, $^1J(PC) = 44.5$ Hz, C_i), 134.52 (d, $^2J(PC) = 10.4$ Hz, C_o), 131.69 (dd, $^1J(PC) = 41.1$ Hz, $^3J(PC) = 1.5$ Hz, C_i), 131.42 (d, $^4J(PC) = 2.4$ Hz, C_p), 131.36 (d, $^4J(PC) = 2.5$ Hz, C_p), 131.29 (d, $^2J(PC) = 9.1$ Hz, C_o), 131.00 (dd, $^2J(PC) = 15.2$ Hz, $^4J(PC) = 0.9$ Hz, C_6), 131.00 (d, $^4J(PC) = 2.5$ Hz, C_p), 130.95 (d, $^2J(PC) = 13.2$ Hz, C_o), 129.42 (d, $^1J(PC) = 50.4$ Hz, C_o), 129.42 (d, $^1J(PC) = 50.4$ Hz, C_i), 129.26 (d, $^3J(PC) = 9.8$ Hz, C_m), 128.63 (d, $^3J(PC) = 10.8$ Hz, C_m), 118.65 (s, Cy), 106.54 (d, $J(PC) = 1.5$ Hz, Cy), 98.21 (dd, $J(PC) = 3.1$, 1.5 Hz, Cy), 95.64 (dd, $J(PC) = 3.0$, 2.0 Hz, Cy), 94.95 (dd, $J(PC) = 4.9$, 2.3 Hz, Cy), 91.62 (d, $J(PC) = 4.3$ Hz, Cy), 57.13 (dd, $^1J(PC) = 36.6$ Hz, $^2J(PC) = 12.7$ Hz, C_1), 48.73 (dd, $^1J(PC) = 33.8$ Hz, $^3J(PC) = 0.6$ Hz, C_4), 31.26 (dd, $^1J(PC) = 39.6$ Hz, $^2J(PC) = 30.3$ Hz, C_2), 30.45 (dd, $^2J(PC) = 10.6$ Hz, $^2J(PC) = 2.2$ Hz, C_3), 29.84 (s, CH), 21.21 (s, CH_3), 20.64 (s, CH_3), 16.77 (s, CH_3), 13.89 (apparent t, $^3J(PC) = {}^4J(PC) = 1.9$ Hz, CH_3), 12.33 (d, $^3J(PC) = 3.5$ Hz, CH_3).

2.2.8. *[(η⁶-p-MeC₆H₄CHMe₂)Ru(DMPP)(PVS)Cl]PF₆ (**8a,b**)*

^{1}H-NMR (499.8 MHz, CD_3NO_2, 25°C) (**8a**) δ 7.82 (m, 2H, H_o, PPh), 7.62 (d, $^3J(HH) = 8.0$ Hz, 2H, H_o, SPh), 7.56 (m, 1H, H_p, PPh), 7.46 (m, 5H, H_m, SPh, PPh, H_p, SPh), 6.48 (d, $^3J(HH) = 6.5$ Hz, 1H, Cy), 6.08 (dd, $^3J(HH) = 6.5$ Hz, $J(PH) = 1.0$ Hz, 1H, Cy), 5.96 (d, $^3J(HH) = 5.5$ Hz, 1H, Cy), 5.65 (d, $^3J(HH) = 5.5$ Hz, 1H, Cy), 4.10 (apparent ddt, $^3J(PH) = 38.5$ Hz, $^3J(H_2H_4) = 9.0$ Hz, $^3J(H_1H_2) = {}^3J(H_2H_3) = 2.0$ Hz, 1H, H_2), 3.71 (dd, $^4J(H_1H_5) = 1.5$ Hz, $^2J(PH) = 1.0$ Hz, 1H, H_5), 3.56 (apparent dt, $^3J(H_1H_2) = 2.0$ Hz, $^4J(H_1H_5) = {}^2J(PH) = 1.5$ Hz, 1H, H_1), 2.45 (sept, $^3J(HH) = 7.0$ Hz, 1H, CH), 2.38 (ddd, $^3J(PH) = 25.0$ Hz, $^2J(H_3H_4) = 14.0$ Hz, $^3J(H_2H_4) = 9.0$ Hz, 1H, H_4), 2.21 (s, 3H, CH_3), 1.93 (dd, $^2J(H_3H_4) = 14.0$ Hz, $^3J(H_2H_3) = 2.0$ Hz, 1H, H_3), 1.68 (s, 3H, CH_3), 1.66 (s, 3H, CH_3), 1.03 (d, $^3J(HH) = 7.0$ Hz, 3H, CH_3), 0.70 (d, $^3J(HH) = 7.0$ Hz, 3H, CH_3). (**8b**) δ 7.93 (d, $^3J(HH) = 8.0$ Hz, 2H, H_o, SPh), 7.80 (m, 2H, H_o, PPh), 7.69 (m, 1H, H_p, PPh), 7.48 (m, 4H, H_m, PPh, SPh), 7.43 (m, 1H, H_p, SPh), 6.10 (d, $^3J(HH) = 6.5$ Hz, 1H, Cy), 5.94 (d, $^3J(HH) = 6.5$ Hz, 1H, Cy), 5.50 (d, $^3J(HH) = 6.0$ Hz, 1H, Cy), 5.42 (d, $^3J(HH) = 6.0$ Hz, 1H, Cy), 3.34 (dd, $^4J(H_1H_5) = 1.5$ Hz, $^2J(PH) = 1.0$ Hz, 1H, H_1), 3.24 (apparent dt, $^3J(H_3H_5) = 2.0$ Hz, $^4J(H_1H_5) = {}^2J(PH) = 1.5$ Hz, 1H, H_5), 2.53 (m, 3H, CH, H_2, H_3), 2.03 (s, 3H, CH_3), 1.82 (ddd, $^3J(PH) = 22.0$ Hz, $^2J(H_3H_4) = 3.0$ Hz, $^3J(H_2H_4) = 7.5$ Hz, 1H, H_4), 1.77 (s, 3H, CH_3), 1.51 (s, 3H, CH_3), 1.22 (d, $^3J(HH) = 7.0$ Hz, 3H, CH_3), 1.08 (d, $^3J(HH) = 7.0$ Hz, 3H, CH_3). $^{13}C\{^1H\}$-NMR (125.7 MHz, CD_3NO_2, 25°C) (**8a**) δ 141.00 (s, C_i, SPh), 132.34 (d, $^2J(PC) = 8.0$ Hz, C_o, PPh), 131.61 (d, $^4J(PC) = 2.5$ Hz, C_p, PPh), 130.10 (s, C_5), 129.16 (s, C_m, SPh), 128.94 (s, C_o, SPh), 128.85 (s, C_6), 128.62 (s, C_p, SPh), 128.60 (d, $^1J(PC) = 46.8$ Hz, C_i, PPh), 128.44 (d, $^3J(PC) = 10.3$ Hz, C_m, PPh), 113.47 (s, Cy), 102.49 (s, Cy), 96.41 (d, $J(PC) = 5.4$ Hz, Cy), 94.57 (d, $J(PC) = 5.9$ Hz, Cy), 88.82 (s, Cy), 85.02 (s, Cy), 55.95 (d, $^1J(PC) = 40.5$ Hz, C_1), 48.11 (d, $^1J(PC) = 28.3$ Hz, C_4), 40.97 (d, $^2J(PC) = 33.6$ Hz, C_2), 33.20 (d, $^2J(PC) = 19.5$ Hz, C_3), 30.86 (s, CH), 21.42 (s, CH_3), 19.46 (s, CH_3), 17.46 (s, CH_3), 13.51 (d, $^3J(PC) = 2.8$ Hz, CH_3), 13.00 (d, $^3J(PC) = 2.3$ Hz, CH_3). (**8b**) δ 140.19 (s, C_i, SPh), 131.73 (d, $^4J(PC) = 2.5$ Hz, C_p, PPh), 131.43 (s, C_m, SPh), 131.04 (d, $^2J(PC) = 6.8$ Hz, C_o, PPh), 130.53 (s, C_5 or C_6), 130.06 (s, C_5 or C_6), 130.00 (d, $^1J(PC) = 44.1$ Hz, C_i, PPh), 129.37 (d, $^3J(PC) = 11.4$ Hz, C_m, PPh), 129.37 (s, C_o, SPh), 114.57 (s, Cy), 102.62 (s, Cy), 96.12 (d, $J(PC) = 5.0$ Hz, Cy), 94.82 (d, $J(PC) = 5.5$ Hz, Cy), 89.94 (s, Cy), 89.07 (s, Cy), 56.13 (d, $^1J(PC) = 34.1$ Hz, C_1), 45.87 (d, $^1J(PC) = 30.8$ Hz, C_4), 43.88 (d, $^2J(PC) = 31.5$ Hz, C_2), 33.05 (d, $^2J(PC) = 14.0$ Hz, C_3), 30.18 (s, CH), 21.54 (s, CH_3), 19.92 (s, CH_3), 16.68 (s, CH_3), 13.76 (d, $^3J(PC) = 1.8$ Hz, CH_3), 12.72 (d, $^3J(PC) = 3.5$ Hz, CH_3).

2.2.9. [(η^6p-$MeC_6H_4CHMe_2$)Ru(DMPP)(PVSO)Cl]PF_6 (**9**)

^{1}H-NMR (499.8 MHz, CD_3NO_2, 25°C) δ 8.38 (m, 2H, H_o, SPh), 7.88 (m, 2H, H_o, PPh), 7.76 (m, 6H, $H_{m,\ p}$ SPh, PPh), 6.14 (dd, ^3J(HH) = 6.5 Hz, ^4J(HH) = 1.5 Hz, 1H, Cy), 6.09 (dd, ^3J(HH) = 6.5 Hz, ^4J(HH) = 1.5 Hz, 1H, Cy), 5.72 (dd, ^3J(HH) = 6.5 Hz, ^4J(HH) = 1.5 Hz, 1H, Cy), 5.59 (dd, ^3J(HH) = 6.5 Hz, ^4J(HH) = 1.5 Hz, 1H, Cy), 4.30 (dddd, ^3J(PH) = 38.0 Hz, $^3J(H_2H_4)$ = 9.5 Hz, $^3J(H_2H_3)$ = 3.1 Hz, $^3J(H_1H_2)$ = 1.0 Hz, 1H, H_2), 4.04 (apparent td, ^2J(PH) = $^4J(H_1H_5)$, 2.2 Hz, $^3J(H_1H_2)$ = 1.0 Hz, 1H, H_1), 3.23 (apparent t, ^2J(PH) = $^4J(H_1H_5)$ = 2.2 Hz, 1H, H_5), 2.31 (sept, ^3J(HH) = 7.0 Hz, 1H, CH), 2.15 (dd, $^2J(H_3H_4)$ = 14.5 Hz, $^3J(H_2H_3)$ = 3.1 Hz, 1H, H_3), 2.13 (s, 3H, CH_3), 1.88 (s, 3H, CH_3), 1.56 (ddd, ^3J(PH) = 22.5 Hz, $^2J(H_3H_4)$ = 14.5 Hz, $^3J(H_2H_4)$ = 9.5 Hz, 1H, H_4), 1.52 (s, 3H, CH_3), 1.19 (d, ^3J(HH) = 7.0 Hz, 3H, CH_3), 1.12 (d, ^3J(HH) = 7.0 Hz, 3H, CH_3). $^{13}C\{^1H\}$-NMR (125.7 MHz, CD_3NO_2, 25°C) δ 140.42 (s, C_5), 140.17 (s, C_6), 134.11 (s, C_o, SPh), 132.35 (d, ^4J(PC) = 2.4 Hz, C_p, PPh), 131.62 (d, ^2J(PC) = 7.2 Hz, C_o, PPh), 129.64 (s, C_m, SPh), 129.57 (d, ^1J(PC) = 20.9 Hz, C_i, PPh), 129.57 (d, ^3J(PC) = 10.6 Hz, C_m, PPh), 128.39 (s, C_i, SPh), 128.04 (s, C_o, SPh), 120.59 (s, Cy), 110.74 (s, Cy), 98.07 (d, J(PC) = 2.9 Hz, Cy), 96.48 (s, Cy), 96.29 (d, J(PC) = 3.6 Hz, Cy), 91.27 (s, Cy), 63.35 (d, ^2J(PC) = 35.1 Hz, C_2), 52.73 (d, ^1J(PC) = 34.3 Hz, C_1), 46.87 (d, ^1J(PC) = 32.9 Hz, C_4), 30.16 (s, CH), 28.66 (d, ^2J(PC) = 11.1 Hz, C_3), 21.32 (s, CH_3), 20.36 (s, CH_3), 17.48 (s, CH_3), 13.90 (d, ^3J(PC) = 1.8 Hz, CH_3), 12.74 (d, ^3J(PC) = 3.5 Hz, CH_3).

2.2.10. [(η^6-p-$MeC_6H_4CHMe_2$)Ru(DMPP)(MVK)-Cl]PF_6 (**10**)

^{1}H-NMR (499.8 MHz, acetone-d_6, 25°C) δ 7.93 (m, 2H, H_o), 7.54 (m, 1H, H_p), 7.47 (m, 2H, H_m), 6.18 (d, ^3J(HH) = 6.5 Hz, 1H, Cy), 6.12 (d, ^3J(HH) = 6.5 Hz, 1H, Cy), 5.88 (m, 2H, Cy), 4.26 (apparent dq, $^3J(H_3H_5)$ = 3.0 Hz, ^2J(PH) = $^3J(H_4H_5)$ = $^4J(H_1H_5)$ = 1.5 Hz, 1H, H_5), 3.47 (dddd, ^3J(PH) = 23.5 Hz, $^3J(H_2H_4)$ = 10.5 Hz, $^3J(H_2H_3)$ = 4.5 Hz, $^3J(H_1H_2)$ = 1.5 Hz, 1H, H_2), 3.17 (apparent q, ^2J(PH) = $^3J(H_1H_2)$ = $^4J(H_1H_5)$ = 1.5 Hz, 1H, H_1), 2.74 (s, 3H, $CH_3C(O)$), 2.42 (apparent ddt, $^2J(H_3H_4)$ = 13.5 Hz, $^3J(H_2H_3)$ = 4.5 Hz, $^3J(H_3H_5)$ = ^3J(PH) = 3.0 Hz, 1H, H_3), 2.32 (quin, ^3J(HH) = 7.0 Hz, 1H, CH), 2.20 (dddd, ^3J(PH) = 32.5 Hz, $^2J(H_3H_4)$ = 13.5 Hz, $^3J(H_2H_4)$ = 10.5 Hz, $^3J(H_4H_5)$ = 1.5 Hz, 1H, H_4), 1.88 (s, 3H, CH_3), 1.71 (m, 3H, CH_3), 1.53 (s, 3H, CH_3), 0.99 (d, ^3J(HH) = 7.0 Hz, 3H, CH_3), 0.84 (d, ^3J(HH) = 7.0 Hz, 3H, CH_3). $^{13}C\{^1H\}$-NMR (125.7 MHz, acetone-d_6, 25°C) 233.05 (d, ^3J(PC) = 1.1 Hz, C=O), 140.46 (s, C_5), 135.13 (d, ^2J(PC) = 1.5 Hz, C_6), 133.14 (d, ^2J(PC) = 7.9 Hz, C_o), 132.18 (d, ^4J(PC) = 2.5 Hz, C_p), 130.27 (d, ^1J(PC) = 47.5 Hz, C_i), 129.29 (d, ^3J(PC) = 9.9 Hz, C_m), 106.34 (s, Cy), 99.79 (s, Cy), 93.01 (d, J(PC) = 5.7 Hz, Cy), 92.07 (d, J(PC) = 4.3 Hz, Cy), 87.78 (d, J(PC) = 0.9 Hz, Cy), 84.72 (d, J(PC) = 3.0 Hz, Cy), 50.91 (d, ^1J(PC) = 29.9 Hz, C_4), 49.53 (d, ^2J(PC) = 16.5 Hz, C_2), 48.15 (d, ^1J(PC) = 32.7 Hz, C_1), 32.25 (s, $CH_3C(O)$), 32.10 (d, ^2J(PC) = 23.5 Hz, C_3), 31.80 (s, CH), 22.34 (s, CH_3), 21.36 (s, CH_3), 18.36 (s, CH_3), 14.52 (d, ^3J(PC) = 2.5 Hz, CH_3), 14.11 (d, ^3J(PC) = 2.3 Hz, CH_3).

2.2.11. [(η^6-p-$MeC_6H_4CHMe_2$)Ru(DMPP)(DMAA)-Cl]PF_6 (**11**)

^{1}H-NMR (499.8 MHz, acetone-d_6, 25°C) δ 7.70 (m, 2H, H_o), 7.30 (m, 1H, H_p), 7.24 (m, 2H, H_m), 5.78 (d, ^3J(HH) = 6.0 Hz, 1H, Cy), 5.76 (d, ^3J(HH) = 6.0 Hz, 1H, Cy), 5.52 (d, ^3J(HH) = 5.5 Hz, 1H, Cy), 5.47 (d, ^3J(HH) = 5.5 Hz, 1H, Cy), 3.91 (dd, $^3J(H_3H_5)$ = 3.5 Hz, ^2J(PH) = 1.5 Hz, 1H, H_5), 3.20 (dddd, ^3J(PH) = 20.5 Hz, $^3J(H_2H_4)$ = 10.0 Hz, $^3J(H_2H_3)$ = 3.5 Hz, $^3J(H_1H_2)$ = 1.5 Hz, 1H, H_2), 3.11 (s, 3H, NCH_3), 2.97 (apparent t, ^2J(PH) = $^3J(H_1H_2)$ = 1.5 Hz, 1H, H_1), 2.93 (s, 3H, NCH_3), 2.13 (apparent dq, $^2J(H_3H_4)$ = 13.0 Hz, $^2J(H_2H_3)$ = ^3J(PH) = $^3J(H_3H_5)$ = 3.5 Hz, 1H, H_3), 2.05 (sept, ^3J(HH) = 7.0 Hz, 1H, CH), 1.84 (ddd, ^3J(PH) = 31.5 Hz, $^2J(H_3H_4)$ = 13.0 Hz, $^3J(H_2H_4)$ = 10.0 Hz, 1H, H_4), 1.61 (s, 3H, CH_3), 1.50 (s, 3H, CH_3), 1.32 (s, 3H, CH_3), 0.79 (d, ^3J(HH) = 7.0 Hz, 3H, CH_3), 0.61 (d, ^3J(HH) = 7.0 Hz, 3H, CH_3). $^{13}C\{^1H\}$-NMR (125.7 MHz, acetone-d_6, 25°C) δ 181.79 (s, C=O), 140.53 (s, C_5), 136.03 (s, C_6), 132.95 (d, ^2J(PC) = 7.4 Hz, C_o), 131.97 (d, ^4J(PC) = 2.6 Hz, C_p), 130.94 (d, ^1J(PC) = 45.4 Hz, C_i), 129.27 (d, ^3J(PC) = 10.1 Hz, C_m), 105.56 (s, Cy), 98.66 (s, Cy), 92.09 (d, J(PC) = 5.7 Hz, Cy), 91.37 (d, J(PC) = 4.4 Hz, Cy), 86.79 (s, Cy), 84.24 (d, J(PC) = 3.1 Hz, Cy), 51.91 (d, ^1J(PC) = 33.2 Hz, C_1), 50.16 (d, ^1J(PC) = 29.2 Hz, C_4), 39.92 (d, ^2J(PC) = 16.3 Hz, C_2), 39.72 (s, NCH_3), 38.51 (s, NCH_3), 31.50 (s, CH), 30.81 (d, ^2J(PC) = 23.4 Hz, C_3), 22.32 (s, CH_3), 21.45 (s, CH_3), 18.24 (s, CH_3), 14.58 (d, ^3J(PC) = 2.6 Hz, CH_3), 14.21 (d, ^3J(PC) = 2.3 Hz, CH_3).

2.2.12. [(η^6-p-$MeC_6H_4CHMe_2$)Ru(DMPP)(2VP)Cl]PF_6 (**12**)

^{1}H-NMR (499.8 MHz, CD_3NO_2, 25°C) δ 9.64 (dd, $^3J(H_aH_b)$ = 6.0 Hz, $^4J(H_aH_c)$ = 1.0 Hz, 1H, H_a), 7.92 (apparent td, $^3J(H_bH_c)$ = $^3J(H_cH_d)$ = 7.5 Hz, $^4J(H_aH_c)$ = 1.0 Hz, 1H, H_c), 7.85 (m, 2H, H_o), 7.53 (m, 1H, H_p), 7.47 (m, 2H, H_m), 7.42 (dd, $^3J(H_cH_d)$ = 7.5 Hz, $^4J(H_bH_d)$ = 1.5 Hz, 1H, H_d), 7.41 (ddd, $^3J(H_bH_c)$ = 7.5 Hz, $^3J(H_aH_b)$ = 6.0 Hz, $^4J(H_bH_d)$ = 1.5 Hz, 1H, H_b), 6.20 (dd, ^3J(HH) = 6.5 Hz, ^4J(HH) = 1.0 Hz, 1H, Cy), 6.06 (d, ^3J(HH) = 6.5 Hz, 1H, Cy), 5.83 (d, ^3J(HH) = 5.5 Hz, 1H, Cy), 5.67 (dd, ^3J(HH) = 5.5 Hz, ^4J(HH) = 1.0 Hz, 1H, Cy), 4.01 (apparent q, $^3J(H_3H_5)$ = $^3J(H_4H_5)$ = $^4J(H_1H_5)$ = 2.0 Hz, 1H, H_5), 3.51 (dddd, ^3J(PH) = 26.0 Hz, $^3J(H_2H_4)$ = 11.0 Hz, $^3J(H_2H_3)$ = 4.0 Hz, $^3J(H_1H_2)$ = 1.0 Hz, 1H, H_2), 2.84

Table 3
Crystallographic data for complexes **1**–**20**

	1	**2**	**3a**
Chemical formula	$C_{38}H_{44}ClF_6P_3Ru{\cdot}C_3H_6O$	$C_{32}H_{39}ClF_6P_2RuS$	$C_{32}H_{39}ClF_6OP_2RuS$
Formula weight	902.24	768.15	784.15
Crystal size (mm)	0.32 × 0.58 × 0.46	0.42 × 0.54 × 0.42	0.24 × 0.44 × 0.34
Crystal system	Triclinic	Orthorhombic	Orthorhombic
Space group	$P\bar{1}$	*Pbca*	*Pca*2/1
a (Å)	11.4409(12)	18.141(3)	21.174(3)
b (Å)	11.5147(7)	11.7518(14)	8.8694(5)
c (Å)	15.5747(9)	30.520(7)	17.8009(11)
α (°)	105.535(4)	90	90
β (°)	91.364(6)	90	90
γ (°)	92.362(6)	90	90
V (Å^3)	1973.9(3)	6506(2)	3343.0(6)
Z	2	8	4
D_{calc} (g cm^{-3})	1.518	1.568	1.558
μ (mm^{-1})	0.648	0.783	0.766
Reflections collected	8034	6990	7329
Unique reflections	6898	5716	3267
max./min. transmission factors	0.9122/0.8127	0.8641/0.6994	0.9245/0.8458
Data/restraints/parameter	6898/0/478	5716/0/389	3267/1/388
Goodness-of-fit	1.028	1.019	1.016
$R_1/wR_2(I>2\sigma(I))$ [a]	0.0358/0.0881	0.0564/0.1371	0.0465/0.0837
	3b	**4**	**5**
Chemical formula	$C_{32}H_{39}ClF_6OP_2RuS$	$C_{28}H_{37}ClF_6OP_2Ru$	$C_{29}H_{40}ClF_6NOP_2Ru$
Formula weight	784.15	702.04	731.08
Crystal size (mm)	0.08 × 0.48 × 0.38	0.32 × 0.52 × 0.42	0.18 × 0.36 × 0.24
Crystal system	Orthorhombic	Triclinic	Monoclinic
Space group	*Pbca*	$P\bar{1}$	$P2_1/c$
a (Å)	16.6306(15)	10.8610(13)	9.2334(7)
b (Å)	19.281(4)	10.8668(13)	21.6872(16)
c (Å)	20.7321(17)	13.9084(19)	15.9245(15)
α (°)	90	93.819(10)	90
β (°)	90	112.246(9)	94.245(7)
γ (°)	90	92.962(9)	90
V (Å^3)	6647.8(15)	1510.7(3)	3176.6(5)
Z	8	2	4
D_{calc} (g cm^{-3})	1.567	1.543	1.529
μ (mm^{-1})	0.771	0.771	0.738
Reflections collected	7061	6234	7073
Unique reflections	5850	5317	5579
max./min. transmission factors	0.9179/0.8272	0.9605/0.5593	0.9929/0.9082
Data/restraints/parameter	5850/0/398	5317/0/352	5579/0/371
Goodness-of-fit	1.004	1.036	1.048
$R_1/wR_2(I>2\sigma(I))$ [a]	0.0676/0.1207	0.0601/0.1388	0.0815/0.1445
	6	**7**	
Chemical formula	$C_{31}H_{38}ClF_6NP_2Ru$	$C_{36}H_{40}ClF_6P_3Ru{\cdot}0.5CH_3NO_2{\cdot}0.5ClCH_2CH_2Cl$	
Formula weight	737.08	896.11	
Crystal size (mm)	0.06 × 0.28 × 0.24	0.16 × 0.38 × 0.24	
Crystal system	Monoclinic	Triclinic	
Space group	$P2_1/c$	$P\bar{1}$	
a (Å)	9.1122(12)	11.3088(13)	
b (Å)	21.744(7)	19.1024(16)	
c (Å)	15.927(3)	19.7843(16)	
α (°)	90	79.550(6)	
β (°)	95.948(18)	86.821(9)	
γ (°)	90	74.795(8)	
V (Å^3)	3138.8(12)	4055.7(7)	
Z	4	4 [b]	
D_{calc} (g cm^{-3})	1.560	1.468	
μ (mm^{-1})	0.745	0.694	
Reflections collected	5427	16619	

Table 3 (*Continued*)

	6	**7**	
Unique reflections	4110	14251	
max./min. transmission factors	0.9674/09114	0.9535/0.9036	
Data/restraints/parameter	4110/0/379	14251/12/919	
Goodness-of-fit	1.019	1.004	
$R_1/wR_2(I>2\sigma(I))$ [a]	0.0703/0.1384	0.0788/0.1524	
	8	**9**	**10**
Chemical formula	$C_{30}H_{35}ClF_6P_2RuS$	$C_{30}H_{35}ClF_6OP_2RuS \cdot 0.5H_2O$	$C_{26}H_{33}ClF_6OP_2Ru$
Formula weight	740.10	764.10	673.98
Crystal size (mm)	0.16 × 0.36 × 0.36	0.18 × 0.42 × 0.28	0.22 × 0.44 × 0.38
Crystal system	Monoclinic	Triclinic	Monoclinic
Space group	$P2_1/c$	$P\bar{1}$	$P2_1/n$
a (Å)	10.5288(17)	10.9698(13)	11.3782(12)
b (Å)	17.834(3)	12.4647(12)	11.1224(15)
c (Å)	16.828(3)	12.6210(10)	22.628(3)
α (°)	90	84.908(7)	90
β (°)	98.263(17)	74.074(9)	94.219(9)
γ (°)	90	82.634(8)	90
V (Å^3)	3127.1(10)	1643.2(3)	2855.8(6)
Z	4	2	4
D_{calc} (g cm^{-3})	1.572	1.544	1.568
μ (mm^{-1})	0.812	0.778	0.812
Reflections collected	6923	6751	6496
Unique reflections	5511	5759	5026
max./min. transmission factors	0.9553/0.8161	0.9685/0.8939	0.9302/0.8758
Data/restraints/parameter	5511/0/370	5410/0/389	5026/0/334
Goodness-of-fit	1.006	1.025	1.016
$R_1/wR_2(I>2\sigma(I))$ [a]	0.0771/0.1319	0.0408/0.0907	0.0589/0.1128
	11	**12**	**13**
Chemical formula	$C_{27}H_{36}ClF_6NOP_2Ru$	$C_{29}H_{34}ClF_6NP_2Ru \cdot 0.5C_3H_6O$	$C_{32}H_{32}ClF_6P_3Ru$
Formula weight	703.03	738.07	760.01
Crystal size (mm)	0.14 × 0.44 × 0.38	0.44 × 0.38 × 0.22	0.03 × 0.54 × 0.20
Crystal system	Triclinic	Orthorhombic	Monoclinic
Space group	$P\bar{1}$	$Pbcn$	$P2_1/c$
a (Å)	10.813(3)	23.799(4)	12.765(3)
b (Å)	11.219(3)	14.707(2)	12.0998(9)
c (Å)	14.517(6)	20.662(4)	21.354(4)
α (°)	112.31(3)	90	90
β (°)	105.97(2)	90	106.658(14)
γ (°)	93.72(2)	90	90
V (Å^3)	1537.8(8)	7232(2)	3159.8(9)
Z	2	8	4
D_{calc} (g cm^{-3})	1.518	1.356	1.598
μ (mm^{-1})	0.759	0.648	0.791
Reflections collected	6067	7689	7039
Unique reflections	5200	6361	5573
max./min. transmission factors	0.9398/0.7410	0.917/0.801	0.9189/0.8162
Data/restraints/parameter	5200/0/352	6361/0/398	5573/0/388
Goodness-of-fit	1.081	1.005	1.004
$R_1/wR_2(I>2\sigma(I))$ [a]	0.0965/0.2445	0.0844/0.1949	0.0750/0.1141
	14	**16**	**17**
Chemical formula	$C_{26}H_{27}ClF_6P_2RuS$	$C_{33}H_{34}ClF_6P_3Ru$	$C_{27}H_{29}ClF_6P_2RuS$
Formula weight	684.00	774.03	698.02
Crystal size (mm)	0.34 × 0.58 × 0.42	0.09 × 0.54 × 0.46	0.20 × 0.38 × 0.24
Crystal system	Monoclinic	Monoclinic	Monoclinic
Space group	$P2_1/c$	$P2_1/c$	$P2_1/c$
a (Å)	11.292(3)	12.8105(9)	10.9290(9)
b (Å)	10.3131(15)	12.1936(9)	10.4534(5)
c (Å)	24.586(5)	21.6418(14)	25.4614(18)
α (°)	90	90	90
β (°)	91.356(14)	106.491(5)	90.368(7)
γ (°)	90	90	90

Table 3 (*Continued*)

	14	**16**	**17**
V (Å^3)	2862.3(11)	3241.5(4)	2908.8(3)
Z	4	4	4
D_{calc} (g cm^{-3})	1.587	1.586	1.594
μ (mm^{-1})	0.880	0.772	0.867
Reflections collected	6556	7206	6680
Unique reflections	5025	5709	5103
max./min. transmission factors	0.9406/0.7743	0.9925/0.8296	0.8911/0.8729
Data/restraints/parameter	5025/0/335	5709/0/398	5103/0/343
Goodness-of-fit	1.032	1.024	1.017
$R_1/wR_2(I>2\sigma(I))$ [a]	0.0387/0.0965	0.0518/0.1024	0.0722/0.1449
	18	**19**	**20**
Chemical formula	$C_{26}H_{28}ClF_6NP_2Ru$	$C_{39}H_{46}ClF_6P_3Ru\cdot CH_2Cl_2$	$C_{37}H_{42}ClF_6P_3Ru$
Formula weight	666.95	943.11	830.14
Crystal size (mm)	0.18 × 0.40 × 0.32	0.12 × 0.48 × 0.18	0.28 × 0.65 × 0.42
Crystal system	Monoclinic	Triclinic	Orthorhombic
Space group	$P2_1/n$	$P\bar{1}$	$P2_12_12_1$
a (Å)	7.2033(8)	10.4121(16)	14.0082(17)
b (Å)	18.0238(17)	11.1175(14)	15.6153(19)
c (Å)	21.062(3)	18.768(3)	16.444(2)
α (°)	90	98.821(10)	90
β (°)	97.991(12)	99.395(13)	90
γ (°)	90	97.072(13)	90
V (Å^3)	2708.0(5)	2093.5(5)	3597.0(8)
Z	4	2	4
D_{calc} (g cm^{-3})	1.636	1.496	1.533
μ (mm^{-1})	0.854	0.736	0.702
Reflections collected	6406	8682	4443
Unique reflections	4769	7363	4228
Max/min transmission	0.9670/0.8732	0.9644/09384	0.8867/07296
Data/restraints/parameter	4769/0/334	7363/0/478	4228/0/434
Goodness-of-fit	1.038	1.033	1.004
$R_1/wR_2(I>2\sigma(I))$ [a]	0.0601/01315	0.0551/0.1330	0.0273/0.0654

[a] $R_1=\Sigma||F_o|-|F_c|/\Sigma|F_o|$; $wR_2=\{\Sigma[w(F_o^2-F_c^2)^2]/\Sigma[w(F_o)^2]^2\}^{0.5}$.
[b] Two inequivalent cations in the asymmetric unit.

(apparent t, $^3J(H_1H_2)={}^4J(H_1H_5)=2.0$ Hz, 1H, H_1), 2.50 (apparent ddt, $^2J(H_3H_4)=13.0$ Hz, $^3J(H_2H_3)=4.0$ Hz, $^3J(PH)={}^3J(H_3H_5)=2.0$ Hz, 1H, H_3), 2.38 (dddd, $^3J(PH)=32.0$ Hz, $^2J(H_3H_4)=13.0$ Hz, $^3J(H_2H_4)=11.0$ Hz, $^3J(H_4H_5)=2.0$ Hz, 1H, H_4), 2.30 (sept, $^3J(HH)=7.0$ Hz, 1H, CH), 1.75 (s, 3H, CH_3), 1.74 (s, 3H, CH_3), 1.56 (s, 3H, CH_3), 1.02 (d, $^3J(HH)=7.0$ Hz, 3H, CH_3), 0.52 (d, $^3J(HH)=7.0$ Hz, CH_3). $^{13}C\{^1H\}$-NMR (125.7 MHz, CD_3NO_2, 25°C) δ 166.94 (d, $^3J(PC)=1.3$ Hz, C_e), 161.85 (s, C_a), 139.16 (s, C_c), 137.75 (s, C_5), 134.34 (d, $^2J(PC)=0.6$ Hz, C_6), 131.91 (d, $^2J(PC)=7.7$ Hz, C_o), 130.98 (d, $^4J(PC)=2.3$ Hz, C_p), 130.68 (d, $^1J(PC)=47.5$ Hz, C_i), 128.21 (d, $^3J(PC)=10.1$ Hz, C_m), 127.95 (s, C_d), 123.81 (s, C_b), 107.27 (s, Cy), 98.47 (s, Cy), 98.07 (d, $J(PC)=5.5$ Hz, Cy), 95.98 (d, $J(PC)=5.5$ Hz, Cy), 88.56 (s, Cy), 85.41 (s, Cy), 50.10 (d, $^1J(PC)=32.9$ Hz, C_4), 47.44 (d, $^1J(PC)=31.7$ Hz, C_1), 45.90 (d, $^2J(PC)=19.4$ Hz, C_2), 31.91 (d, $^2J(PC)=24.5$ Hz, C_3), 30.75 (s, CH), 21.89 (s, CH_3), 19.02 (s, CH_3), 17.12 (s, CH_3), 13.13 (d, $^3J(PC)=2.9$ Hz, CH_3), 12.82 (d, $^3J(PC)=2.5$ Hz, CH_3).

2.2.13. *[(η^6-C_6H_6)Ru(DMPP)(DPVP)Cl]PF_6 (**13**)*

^1H-NMR (499.8 MHz, CD_3NO_2, 25°C) δ 7.50–8.00 (m, 15H, Ph), 5.65 (s, 6H, η^6-C_6H_6), 3.93 (apparent dt, $^4J(H_1H_5)=2.5$ Hz, $^2J(PH)={}^3J(H_1H_2)=1.5$ Hz, 1H, H_1), 3.53 (apparent dddt, $^3J(PH)=40.5$ Hz, $^3J(H_2H_4)=9.5$ Hz, $^2J(PH)=7.5$ Hz, $^3J(H_1H_2)={}^3J(H_2H_3)=2.5$ Hz, 1H, H_2), 3.27 (ddd, $^3J(H_3H_5)=3.5$ Hz, $^4J(H_1H_5)=1.5$ Hz, $^3J(H_4H_5)=0.5$ Hz, 1H, H_5), 2.41 (dddd, $^3J(PH)=23.5$ Hz, $^2J(H_3H_4)=13.0$ Hz, $^3J(H_3H_5)=3.5$ Hz, $^3J(H_2H_3)=2.5$ Hz, 1H, H_3), 1.88 (s, 3H, CH_3), 1.73 (ddddd, $^3J(PH)=23.0$ Hz, $^3J(PH)=21.0$ Hz, $^2J(H_3H_4)=13.0$ Hz, $^3J(H_2H_4)=9.5$ Hz, $^3J(H_4H_5)=0.5$ Hz, 1H, H_4), 1.59 (s, 3H, CH_3). $^{13}C\{^1H\}$-NMR (125.7 MHz, CD_3NO_2, 25°C) δ 138.95 (dd, $^2J(PC)=2.4$ Hz, $^3J(PC)=1.1$ Hz, C_5), 135.07 (d, $^1J(PC)=45.5$ Hz, C_i), 134.77 (d, $^2J(PC)=9.8$ Hz, C_o), 131.90 (dd, $^1J(PC)=42.9$ Hz, $^3J(PC)=1.3$ Hz, C_i), 131.57 (d, $^4J(PC)=2.6$ Hz, C_p), 131.46 (d, $^4J(PC)=2.4$ Hz, C_p), 131.34 (dd, $^2J(PC)=15.8$ Hz, $^3J(PC)=1.3$ Hz, C_6), 131.04 (d, $^4J(PC)=2.8$ Hz, C_p), 130.96 (d, $^2J(PC)=9.0$ Hz, C_o), 129.18 (d, $^3J(PC)=9.9$ Hz, C_m), 129.10 (bd, $^3J(PC)=9.2$ Hz, C_m), 128.74 (d, $^3J(PC)=$

Table 4
Bond lengths (Å) and bond angles (°) For complexes **1**–**20**

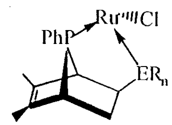

(A)

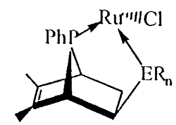

(B)

Compound	Ru–P_1	Ru–P_2 Ru–E	Ru–Cl	Ru–C, (ave.)	P_1–Ru–P_2, P_1–Ru–E	P_1–Ru–Cl	P_2–Ru–Cl, E–Ru–Cl	Diastereomer	Σ∠'s	Arene, P–E–Cl, dihedral angle
(**1**)	2.2964(9)	2.3407(9)	2.4001(9)	2.289(4)	79.84(3)	86.99(3)	89.44(3)	B	256.27	5.6
(**2**)	2.300(2)	2.376(2)	2.408(2)	2.247(6)	82.10(6)	85.94(6)	89.55(6)	A	257.59	2.2
(**3a**)	2.315(2)	2.297(2)	2.403(3)	2.281(10)	79.73(8)	87.78(9)	97.71(9)	B	265.22	7.2
(**3b**)	2.299(2)	2.297(2)	2.376(2)	2.270(9)	81.68(8)	83.33(8)	89.03(8)	A	254.04	3.3
(**4**)	2.305(2)	2.126(4)	2.405(2)	2.227(7)	87.93(12)	85.54(6)	82.76(13)	A	256.23	5.1
(**5**)	2.310(3)	2.120(7)	2.400(3)	2.208(12)	86.8(2)	84.24(10)	83.60(3)	A	254.64	6.7
(**6**)	2.297(3)	2.178(9)	2.394(3)	2.257(12)	88.30(3)	86.19(11)	82.50(3)	A	256.99	1.4
(**7**)	2.307(3)	2.332(2)	2.389(3)	2.266(10)	79.75(9)	88.01(9)	89.95(9)	B	257.71	2.9
(**8**)	2.284(3)	2.379(3)	2.392(3)	2.240(10)	80.50(10)	87.52(10)	95.67(9)	B	263.69	1.3
(**9**)	2.2914(11)	2.2932(10)	2.3994(11)	2.271(4)	79.68(4)	86.47(4)	95.17(4)	B	261.32	1.7
(**10**)	2.284(2)	2.130(4)	2.388(2)	2.207(7)	87.43(13)	82.79(1)	83.31(14)	A	253.53	4.1
(**11**)	2.299(3)	2.112(8)	2.391(4)	2.205(13)	87.5(2)	84.09(14)	84.0(3)	A	255.59	5.5
(**12**)	2.281(3)	2.142(9)	2.387(3)	2.234(12)	88.2(2)	83.45(11)	83.2(3)	A	254.85	2.7
(**13**)	2.282(3)	2.317(3)	2.386(2)	2.255(10)	80.34(9)	88.56(9)	90.52(9)	B	259.42	1.4
(**14**)	2.284(1)	2.386(1)	2.378(1)	2.221(5)	82.06(4)	82.58(4)	90.97(4)	A	255.61	0.5
(**16**)	2.290(2)	2.317(2)	2.3876(14)	2.256(7)	80.15(6)	88.12(6)	91.27(6)	B	259.54	2.0
(**17**)	2.291(2)	2.386(2)	2.378(2)	2.229(10)	81.97(9)	82.61(8)	91.53(8)	A	256.11	0.2
(**18**)	2.276(2)	2.150(6)	2.411(2)	2.238(8)	89.30(16)	84.70(6)	83.37(16)	A	257.37	4.3
(**19**)	2.333(2)	2.365(2)	2.403(2)	2.297(6)	93.00(5)	82.41(5)	87.65(5)		263.06	3.9
(**20**)	2.328(1)	2.357(1)	2.402(1)	2.268(5)	92.89(4)	85.37(4)	88.37(4)		266.63	0.9

10.7 Hz, C_m), 128.24 (d, ^1J(PC) = 51.7 Hz, C_i), 95.62 (t, J(PC) = 2.3 Hz, η^6-C_6H_6), 57.44 (dd, ^1J(PC) = 37.3 Hz, ^2J(PC) = 12.6 Hz, C_1), 47.65 (dd, ^1J(PC) = 33.7 Hz, ^3J(PC) = 1.8 Hz, C_4), 31.08 (dd, ^1J(PC) = 39.2 Hz, ^2J(PC) = 30.7 Hz, C_2), 30.23 (dd, ^2J(PC) = 11.2 Hz, ^2J(PC) = 2.1 Hz, C_3), 13.84 (apparent t, ^3J(PC) = ^4J(PC) = 2.1 Hz, CH_3), 12.37 (d, ^3J(PC) = 3.6 Hz, CH_3).

2.2.14. *[(η^6-C_6H_6)Ru(DMPP)(PVS)Cl]PF_6* (***14***)

^{1}H-NMR (499.8 MHz, CD_3NO_2, 25°C) δ 7.81 (m, 2H, H_o, PPh), 7.63 (m, 2H, H_o, SPh), 7.58 (m, 1H, H_p, PPh), 7.48 (m, 4H, H_m, SPh, PPh), 7.43 (m, 1H, H_p, SPh), 6.15 (d, J(PH) = 0.5 Hz, 6H, η^6-C_6H_6), 4.08 (apparent ddt, ^3J(PH) = 38.5 Hz, $^3J(H_2H_4)$ = 9.2 Hz, $^3J(H_1H_2)$ = $^3J(H_2H_3)$ = 2.0 Hz, 1H, H_2), 3.71 (apparent dq, $^3J(H_3H_5)$ = 3.5 Hz, $^3J(H_4H_5)$ = ^2J(PH) = $^4J(H_1H_5)$ = 2.0 Hz, 1H, H_5), 3.56 (apparent q, ^2J(PH) = $^3J(H_1H_2)$ = $^4J(H_1H_5)$ = 2.0 Hz, 1H, H_1), 2.39 (dddd, ^3J(PH) = 25.0 Hz, $^2J(H_3H_4)$ = 14.0 Hz, $^3J(H_2H_4)$ = 9.2 Hz, $^3J(H_4H_5)$ = 2.0 Hz, 1H, H_4), 2.03 (ddd, $^2J(H_3H_4)$ = 14.0 Hz, $^3J(H_3H_5)$ = 3.5 Hz, $^3J(H_2H_3)$ = 2.0 Hz, 1H, H_3), 1.69 (s, 3H, CH_3), 1.66 (s, 3H, CH_3). $^{13}C\{^1H\}$-NMR (125.7 MHz, CD_3NO_2, 25°C) δ 140.77 (s, C_5), 132.26 (d, ^2J(PC) = 8.2 Hz, C_o, PPh), 131.62 (d, ^4J(PC) = 2.0 Hz, C_p, PPh), 129.92 (s, C_6), 129.15 (s, C_m, SPh), 129.09 (s, C_o, SPh), 128.59 (d, ^1J(PC) = 47.8 Hz, C_i, PPh), 128.58 (s, C_p, SPh), 128.49 (d, ^3J(PC) = 10.4 Hz, C_m, PPh), 128.29 (s, C_i, SPh), 91.56 (d, J(PC) = 2.4 Hz, η^6-C_6H_6), 55.51 (d, ^1J(PC) = 41.0 Hz, C_1), 48.74 (d, ^1J(PC) = 28.3 Hz, C_4), 40.64 (d, ^1J(PC) = 33.6 Hz, C_2), 33.27 (d, ^2J(PC) = 19.2 Hz, C_3), 13.47 (d, ^3J(PC) = 3.0 Hz, CH_3), 12.92 (d, ^3J(PC) = 2.6 Hz, CH_3).

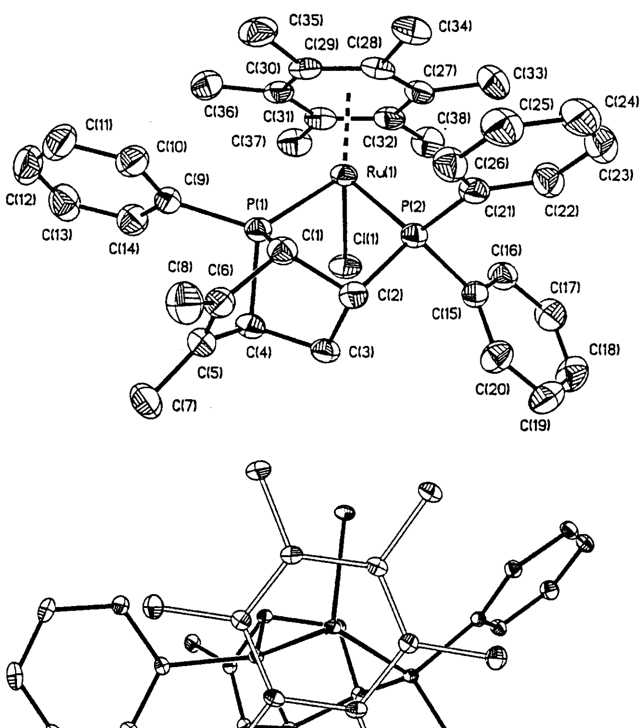

Fig. 1. Two perspectives of the structural drawing of the cation of **1** (hydrogen atoms omitted) showing the atom numbering scheme (40 and 10% probability ellipsoids).

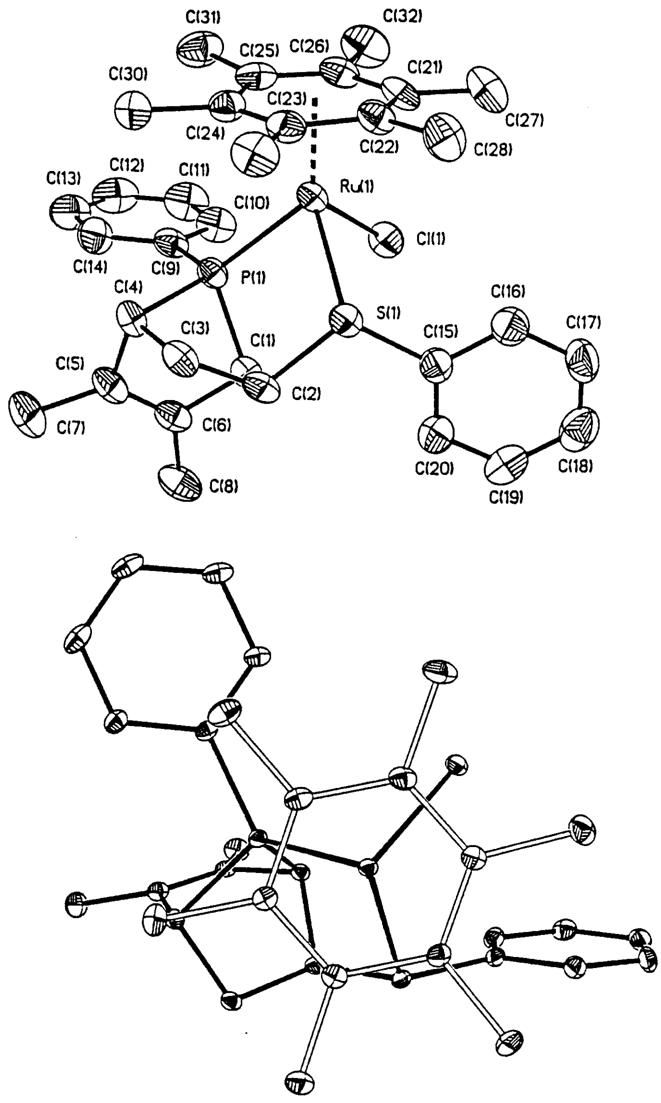

Fig. 2. Two perspectives of the structural drawing of the cation of **2** (hydrogen atoms omitted) showing the atom numbering scheme (40 and 10% probability ellipsoids).

2.2.15. *[(η^6-C_6H_6)Ru(DMPP)(2VP)Cl]PF_6* (***15***)

^{1}H-NMR (499.8 MHz, CD_3NO_2, 25°C) δ 9.67 (dd, $^3J(H_aH_b)$ = 6.0 Hz, $^4J(H_aH_c)$ = 1.5 Hz, 1H, H_a), 7.92 (apparent td, $^3J(H_cH_d)$ = $^3J(H_bH_c)$ = 7.5 Hz, $^4J(H_aH_c)$ = 1.5 Hz, 1H, H_c), 7.86 (m, 2H, H_o, PPh), 7.55 (m, 1H, H_p, PPh), 7.48 (m, 2H, H_m, PPh), 7.41 (dd, $^3J(H_cH_d)$ =

7.5 Hz, $^4J(H_bH_d) = 1.5$ Hz, 1H, H_d), 7.37 (ddd, $^3J(H_bH_c) = 7.5$ Hz, $^3J(H_aH_b) = 6.0$ Hz, $^4J(H_bH_d) = 1.5$ Hz, 1H, H_b), 5.96 (d, $J(PH) = 1.0$ Hz, 6H, η^6-C_6H_6), 4.00 (apparent quin, $^2J(PH) = {}^3J(H_3H_5) = {}^3J(H_4H_5) = {}^4J(H_1H_5) = 1.5$ Hz, 1H, H_5), 3.50 (dddd, $^3J(PH) = 24.5$ Hz, $^3J(H_2H_4) = 11.0$ Hz, $^3J(H_2H_3) = 4.0$ Hz, $^3J(H_1H_2) = 1.5$ Hz, 1H, H_2), 2.86 (apparent t, $^3J(H_1H_2) = {}^4J(H_1H_5) = 1.5$ Hz, 1H, H_1), 2.60 (apparent ddt, $^2J(H_3H_4) = 13.0$ Hz, $^3J(H_2H_3) = 4.0$ Hz, $^3J(PH) = 2.0$ Hz, 1H, H_3), 2.35 (dddd, $^3J(PH) = 32.5$ Hz, $^2J(H_3H_4) = 13.0$ Hz, $^3J(H_2H_4) = 11.0$ Hz, $^3J(H_4H_5) = 1.5$ Hz, 1H, H_4), 1.74 (apparent quin, $^4J(PH) = {}^5J(HH) = 1.0$ Hz, 3H, CH_3), 1.60 (apparent quin, $^4J(PH) = {}^5J(HH) = 1.0$ Hz, 3H, CH_3). $^{13}C\{^1H\}$-NMR (125.7 MHz, CD_3NO_2, 25°C) δ 167.06 (s, C_a), 161.18 (d, $^3J(PC) = 26.4$ Hz, C_e), 139.32 (s, C_c), 137.52 (s, C_5), 134.40 (s, C_6), 131.86 (d, $^2J(PC) = 8.0$ Hz, C_o), 131.13 (d, $^4J(PC) = 2.5$ Hz, C_p), 130.74 (d, $^1J(PC) = 48.0$ Hz, C_i), 128.35 (d, $^3J(PC) = 10.2$ Hz, C_m), 127.92 (s, C_d), 123.69 (s, C_b), 91.19 (d, $J(PC) = 2.5$ Hz, η^6-C_6H_6), 51.07 (d, $^1J(PC) = 33.3$ Hz, C_4), 47.38 (d, $^1J(PC) = 33.3$ Hz, C_1), 45.84 (d, $^2J(PC) = 19.7$ Hz, C_2), 30.02 (d, $^2J(PC) = 25.0$ Hz, C_3), 13.03 (d, $^3J(PC) = 3.1$ Hz, CH_3), 12.74 (d, $^3J(PC) = 2.4$ Hz, CH_3).

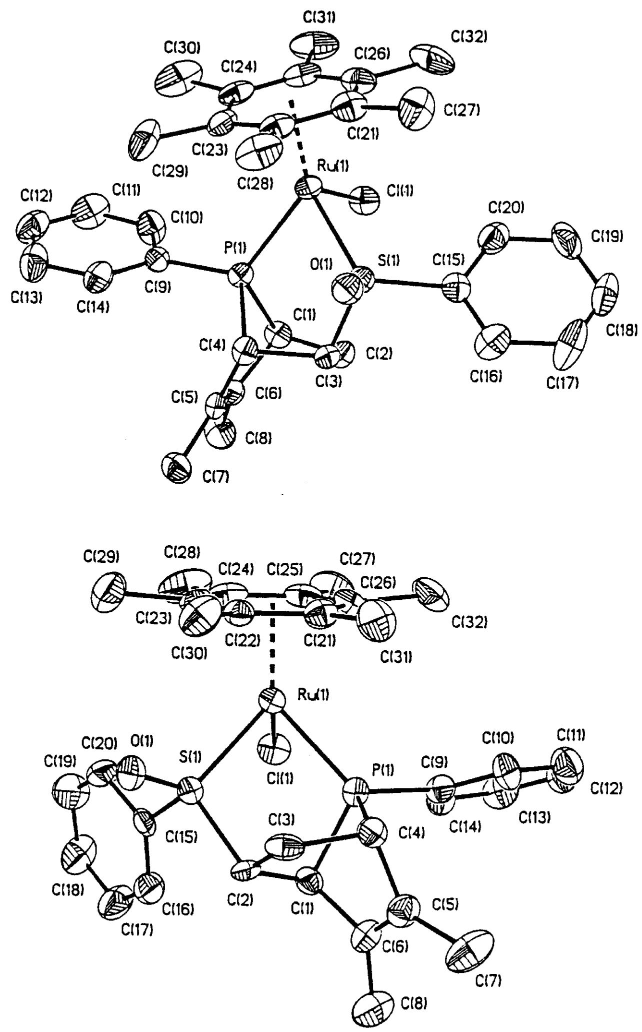

Fig. 3. Structural drawings of the cations of **3a** (top) and **3b** (bottom), (hydrogen atoms omitted) showing the atom numbering scheme (40% probability ellipsoids).

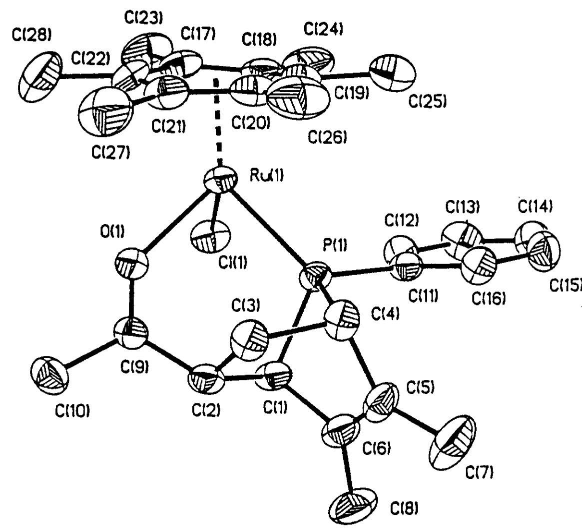

Fig. 4. Structural drawing of the cation of **4** (hydrogen atoms omitted) showing the atom numbering scheme (40% probability ellipsoids).

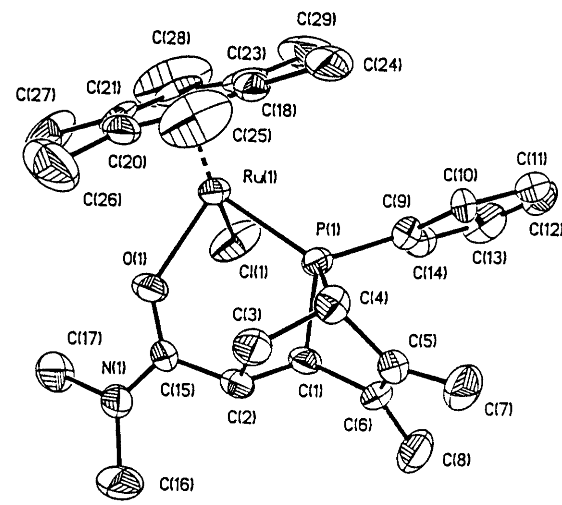

Fig. 5. Structural drawing of the cation of **5** (hydrogen atoms omitted) showing the atom numbering scheme (40% probability ellipsoids).

2.2.16. *[(η^6-MeC$_6$H$_5$)Ru(DMPP)(DPVP)Cl]PF$_6$* (**16**)

^{1}H-NMR (499.8 MHz, CD_3NO_2, 25°C) δ 7.47–7.95 (m, 15H, Ph), 6.31 (d, $^3J(HH) = 6.0$ Hz, 1H, tol), 5.41 (td, $^3J(HH) = 6.0$ Hz, $J(PH) = 2.5$ Hz, 1H, tol), 5.38 (d, $^3J(HH) = 6.0$ Hz, 1H, tol), 5.15 (td, $^3J(HH) = 6.0$ Hz, $J(PH) = 2.5$ Hz, 1H, tol), 4.54 (t, $^3J(HH) = 6.0$ Hz, 1H, tol), 3.92 (apparent td, $^3J(H_1H_2) = {}^2J(PH) = 1.5$ Hz, $^4J(H_1H_5) = 0.6$ Hz, 1H, H_1), 3.51 (apparent dddt, $^3J(PH) = 41.5$ Hz, $^2J(PH) = 9.5$ Hz, $^3J(H_2H_4) = 8.3$ Hz,

$^3J(H_2H_3) = 1.5$ Hz, $^3J(H_1H_2) = 1.5$ Hz, 1H, H_2), 3.26 (apparent ddt, $^3J(H_3H_5) = 3.5$ Hz, $^2J(PH) = 2.0$ Hz, $^4J(H_1H_5) = {}^3J(H_4H_5) = 0.6$ Hz, 1H, H_5), 2.45 (dddd, $^3J(PH) = 23.5$ Hz, $^2J(H_3H_4) = 13.0$ Hz, $^3J(H_3H_5) =$ 3.5Hz, $^3J(H_2H_3) = 1.5$ Hz, 1H, H_3), 2.22 (s, 3H, CH_3), 1.88 (s, 3H, CH_3), 1.72 (ddddd, $^3J(PH) = 23.5$ Hz, $^3J(PH) = 21.5$ Hz, $^2J(H_3H_4) = 13.0$ Hz, $^3J(H_2H_4) = 8.3$ Hz, $^3J(H_4H_5) = 0.6$ Hz, 1H, H_4), 1.53 (s, 3H, CH_3). $^{13}C\{^1H\}$-NMR (125.7 MHz, CD_3NO_2, 25°C) δ 138.97 (dd, $^2J(PC) = 2.5$ Hz, $^3J(PC) = 1.3$ Hz, C_5), 135.12 (d, $^1J(PC) = 45.4$ Hz, C_i), 134.66 (d, $^2J(PC) = 10.2$ Hz, C_o), 132.19 (dd, $^1J(PC) = 42.9$ Hz, $^3J(PC) = 1.4$ Hz, C_i), 131.50 (d, $^4J(PC) = 2.5$ Hz, C_p), 131.38 (d, $^4J(PC) = 2.4$ Hz, C_p), 131.21 (dd, $^2J(PC) = 16.8$ Hz, $^3J(PC) = 1.1$

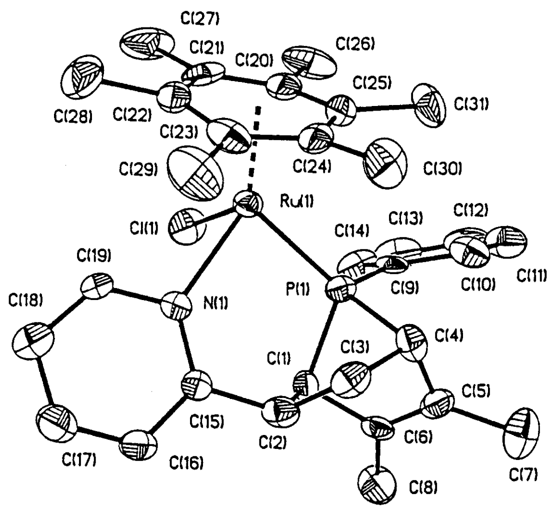

Fig. 6. Structural drawing of the cation of **6** (hydrogen atoms omitted) showing the atom numbering scheme (40% probability ellipsoids).

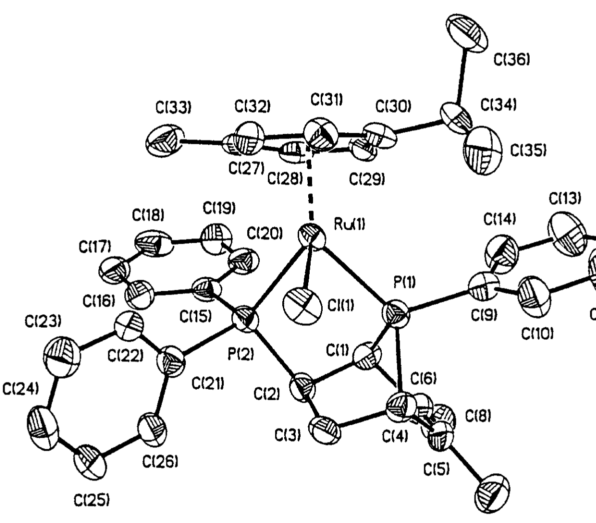

Fig. 7. Structural drawing of the cation of **7** (hydrogen atoms omitted) showing the atom numbering scheme (40% probability ellipsoids).

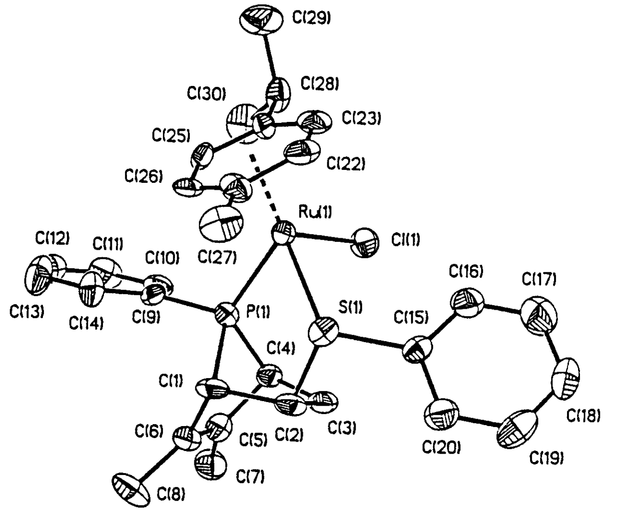

Fig. 8. Structural drawing of the cation of **8** (hydrogen atoms omitted) showing the atom numbering scheme (40% probability ellipsoids).

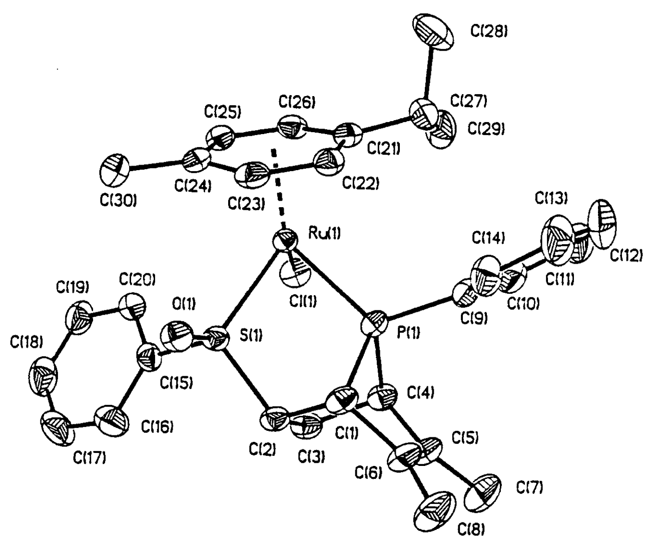

Fig. 9. Structural drawing of the cation of **9** (hydrogen atoms omitted) showing the atom numbering scheme (40% probability ellipsoids).

Hz, C_6), 130.97 (d, $^4J(PC) = 2.9$ Hz, C_p), 130.97 (d, $^2J(PC) = 9.1$ Hz, C_o), 130.82 (bd, $^2J(PC) = 9.1$ Hz, C_o), 129.16 (d, $^3J(PC) = 9.9$ Hz, C_m), 129.10 (bd, $^3J(PC) =$ 9.9 Hz, C_m), 128.70 (d, $^3J(PC) = 10.9$ Hz, C_m), 128.54 (d, $^1J(PC) = 51.3$ Hz, C_i), 116.99 (apparent t, $J(PC) =$ 2.6 Hz, tol), 99.77 (d, $J(PC) = 7.5$ Hz, tol), 98.92 (d, $J(PC) = 7.0$ Hz, tol), 94.78 (d, $J(PC) = 2.9$ Hz, tol), 92.72 (d, $J(PC) = 2.9$ Hz, tol), 82.07 (s, tol), 57.44 (dd, $^1J(PC) = 37.3$ Hz, $^2J(PC) = 12.9$ Hz, C_1), 47.89 (d, $^1J(PC) = 33.1$ Hz, C_4), 31.19 (dd, $^1J(PC) = 39.3$ Hz, $^2J(PC) = 31.0$ Hz, C_2), 30.35 (dd, $^2J(PC) = 11.2$ Hz, $^3J(PC) = 2.0$ Hz, C_3), 17.76 (s, CH_3), 13.88 (apparent t, $^3J(PC) = {}^4J(PC) = 1.9$ Hz, CH_3), 12.39 (d, $^3J(PC) = 3.3$ Hz, CH_3).

2.2.17. *[(η⁶-MeC₆H₅)Ru(DMPP)(PVS)Cl]PF₆* (**17**)

^{1}H-NMR (499.8 MHz, CD_3NO_2, 25°C) δ 7.82 (m, 2H, H_o, PPh), 7.60 (m, 2H, H_o, SPh), 7.56 (m, 1H, H_p, PPh), 7.49 (m, 4H, H_m, PPh, SPh), 7.43 (m, H_p, SPh), 6.26 (apparent t, ^3J(HH) = 5.7 Hz, 1H, tol), 6.21 (d, ^3J(HH) = 5.7 Hz, 1H, tol), 6.09 (apparent t, ^3J(HH) = 5.7 Hz, 1H, tol), 5.71 (d, ^3J(HH) = 5.5 Hz, 1H, tol), 5.70 (dd, ^3J(HH) = 5.7 Hz, ^3J(HH) = 5.5 Hz, 1H, tol), 4.08 (apparent ddt, ^3J(PH) = 38.0 Hz, $^3J(H_2H_4)$ = 9.0 Hz, $^3J(H_1H_2)$ = $^3J(H_2H_3)$ = 2.0 Hz, 1H, H_2), 3.71 (apparent td, $^3J(H_1H_5)$ = ^2J(PH) = 2.0 Hz, $^3J(H_4H_5)$ = 1.0 Hz, 1H, H_5), 3.56 (apparent q, $^3J(H_1H_2)$ = ^2J(PH) = $^4J(H_1H_5)$ = 2.0 Hz, 1H, H_1), 2.37 (dddd, ^3J(PH) = 25.0 Hz, $^2J(H_3H_4)$ = 14.0 Hz, $^3J(H_2H_4)$ = 9.0 Hz, $^3J(H_4H_5)$ = 1.0 Hz, 1H, H_4), 2.16 (s, 3H, CH_3), 2.02 (dd, $^2J(H_3H_4)$ = 14.0 Hz, $^3J(H_2H_3)$ = 2.0 Hz, 1H, H_3), 1.69 (d, ^4J(PH) = 1.0 Hz, 3H, CH_3), 1.68 (d, ^4J(PH) = 1.0 Hz, 3H, CH_3). $^{13}C\{^1H\}$-NMR (125.7 MHz, CD_3NO_2, 25°C) δ 140.75 (s, C_5), 132.26 (d, ^2J(PC) = 8.3 Hz, C_o, PPh), 136.53 (d, ^4J(PC) = 2.6 Hz, C_p, PPh), 129.88 (s, C_6), 129.13 (s, C_m, SPh), 128.90 (s, C_o, SPh), 128.61 (d, ^1J(PC) = 46.9 Hz, C_i, PPh), 128.52 (s, C_p, SPh), 128.50 (s, C_i, SPh), 128.41 (d, ^3J(PC) = 10.3 Hz, C_m, PPh), 112.30 (d, J(PC) = 2.8 Hz, tol), 92.79 (d, J(PC) = 5.5 Hz, tol), 92.22 (d, J(PC) = 2.1 Hz, tol), 91.33 (s, tol), 90.29 (d, J(PC) = 2.0 Hz, tol), 82.63 (s, tol), 55.79 (d, ^1J(PC) = 40.6 Hz, C_1), 48.49 (d, ^1J(PC) = 28.4 Hz, C_4), 40.76 (d, ^2J(PC) = 33.6 Hz, C_2), 33.27 (d, ^2J(PC) = 19.2 Hz, C_3), 17.92 (s, CH_3), 13.49 (d, ^3J(PC) = 2.8 Hz, CH_3), 12.94 (d, ^3J(PC) = 2.5 Hz, CH_3).

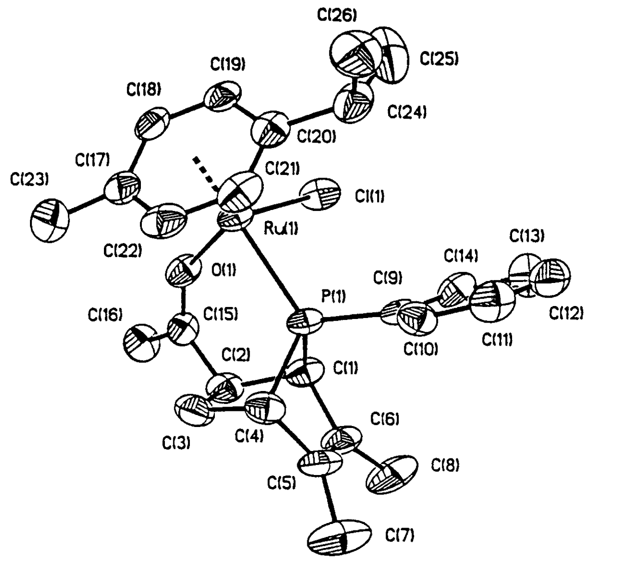

Fig. 10. Structural drawing of the cation of **10** (hydrogen atoms omitted) showing the atom numbering scheme (40% probability ellipsoids).

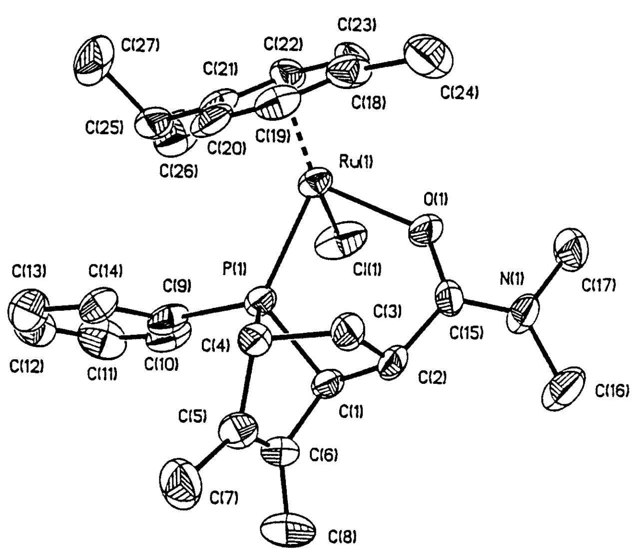

Fig. 11. Structural drawing of the cation of **11** (hydrogen atoms omitted) showing the atom numbering scheme (40% probability ellipsoids).

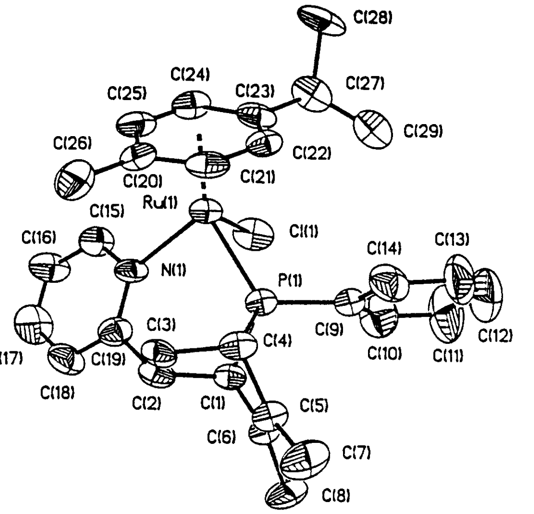

Fig. 12. Structural drawing of the cation of **12** (hydrogen atoms omitted) showing the atom numbering scheme (40% probability ellipsoids).

2.2.18. *[(η⁶-MeC₆H₅)Ru(DMPP)(2VP)Cl]PF₆* (**18**)

^{1}H-NMR (499.8 MHz, CD_3NO_2, 25°C) δ 9.53 (dd, $^3J(H_aH_b)$ = 6.0 Hz, $^4J(H_aH_c)$ = 1.5 Hz, 1H, H_a), 7.91 (apparent td, $^3J(H_bH_c)$ = $^3J(H_cH_d)$ = 7.5 Hz, $^4J(H_aH_c)$ = 1.5 Hz, 1H, H_c), 7.86 (m, 2H, H_o), 7.54 (m, 1H, H_p), 7.48 (m, 2H, H_m), 7.40 (dd, $^3J(H_cH_d)$ = 7.5 Hz, $^4J(H_bH_d)$ = 1.5 Hz, 1H, H_d), 7.37 (ddd, $^3J(H_bH_c)$ = 7.5 Hz, $^3J(H_aH_b)$ = 6.0 Hz, $^4J(H_bH_d)$ = 1.5 Hz, 1H, H_b), 6.13 (d, ^3J(HH) = 6.0 Hz, 1H, tol), 6.09 (apparent t, ^3J(HH) = 6.0 Hz, 1H, tol), 5.96 (apparent td, ^3J(HH) = 6.0 Hz, J(PH) = 1.5 Hz, 1H, tol), 5.49 (apparent t, ^3J(HH) = 6.0 Hz, 1H, tol), 5.15 (d, ^3J(HH) = 6.0 Hz, 1H, tol), 3.97 (apparent dq, $^3J(H_3H_5)$ = 2.0 Hz, ^2J(PH) = $^3J(H_4H_5)$ = $^4J(H_1H_5)$ = 1.5 Hz, 1H, H_5), 3.50 (dddd, ^3J(PH) = 27.0 Hz, $^3J(H_2H_4)$ = 10.7 Hz, $^3J(H_2H_3)$ = 4.0 Hz, $^3J(H_1H_2)$ = 1.5 Hz, 1H, H_2), 2.86 (apparent t, $^3J(H_1H_2)$ = $^4J(H_1H_5)$ = 1.5 Hz, 1H, H_1), 2.57 (apparent

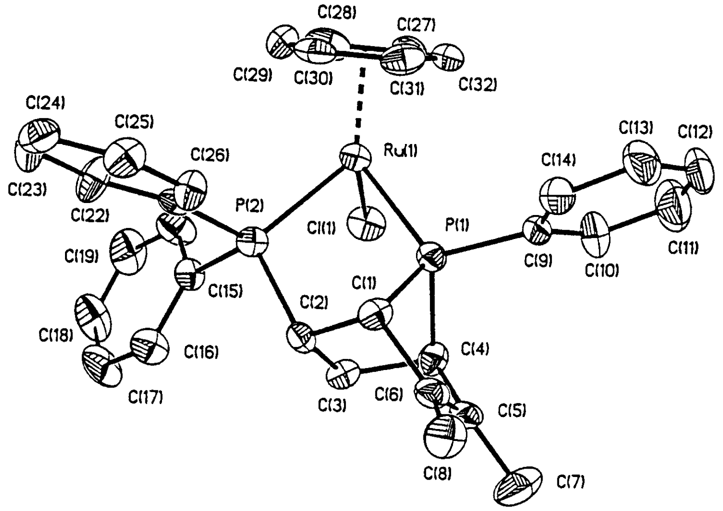

Fig. 13. Structural drawing of the cation of **13** (hydrogen atoms omitted) showing the atom numbering scheme (40% probability ellipsoids).

ddt, $^2J(H_3H_4) = 13.0$ Hz, $^3J(H_2H_3) = 4.0$ Hz, $^3J(H_3H_5) = {}^3J(PH) = 2.0$ Hz, 1H, H_3), 2.34 (dddd, $^3J(PH) = 32.5$ Hz, $^2J(H_3H_4) = 13.0$ Hz, $^3J(H_2H_4) = 10.7$ Hz, $^3J(H_4H_5) = 1.5$ Hz, 1H, H_4), 2.02 (s, 3H, CH_3), 1.75 (s, 3H, CH_3), 1.59 (s, 3H, CH_3). $^{13}C\{^1H\}$-NMR (125.7 MHz, CD_3NO_2, 25°C) δ 167.08 (s, C_a), 161.67 (d, $^3J(PC) = 23.0$ Hz, C_e), 139.24 (s, C_c), 137.50 (s, C_5), 134.35 (s, C_6), 131.85 (d, $^2J(PC) = 7.7$ Hz, C_o), 131.05 (d, $^4J(PC) = 2.1$ Hz, C_p), 130.87 (d, $^1J(PC) = 47.9$ Hz, C_i), 128.29 (d, $^3J(PC) = 9.8$ Hz, C_m), 127.83 (s, C_d), 123.82 (s, C_b), 111.85 (d, $J(PC) = 3.4$ Hz, tol), 96.95 (d, $J(PC) = 6.7$ Hz, tol), 93.72 (d, $J(PC) = 2.1$ Hz, tol), 89.79 (s, tol), 85.83 (d, $J(PC) = 1.8$ Hz, tol), 80.45 (s, tol), 50.71 (d, $^1J(PC) = 33.2$ Hz, C_4), 47.54 (d, $^1J(PC) = 31.8$ Hz, C_1), 45.93 (d, $^2J(PC) = 19.5$ Hz, C_2), 32.07 (d, $^2J(PC) = 24.5$ Hz, C_3), 17.70 (s, CH_3), 13.03 (d, $^3J(PC) = 2.8$ Hz, CH_3), 12.73 (d, $^3J(PC) = 2.4$ Hz, CH_3).

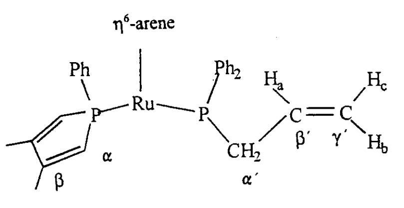

2.2.19. [(η^6-C_6Me_6)Ru(DMPP)(ADPP)Cl]PF_6 (**19**)

^1H-NMR (499.8 MHz, $CDCl_3$, 25°C) δ 7.14–7.64 (m, 15H, Ph), 6.80 (d, $^2J(PH) = 32.5$ Hz, H_α), 6.62 (d, $^2J(PH) = 30.5$ Hz, H_α), 5.00 (apparent dtt, $^3J(H_aH_b) = 15.5$ Hz, $^3J(H_aH_c) = {}^3J(PH) = 10.0$ Hz, $^3J(CH_2H_a) = 5.0$ Hz, 1H, H_a), 4.79 (d, $^3J(H_aH_c) = 10.0$ Hz, 1H, H_c), 4.44 (d, $^3J(H_aH_b) = 15.5$ Hz, 1H, H_b), 3.52 (m, 2H, CH_2), 2.04 (s, 3H, CH_3), 1.90 (s, 3H, CH_3), 1.64 (s, 18H, η^6-C_6Me_6). $^{13}C\{^1H\}$-NMR (125.7 MHz, $CDCl_3$, 25°C) δ 152.86 (d, $^2J(PC) = 5.5$ Hz, C_β), 151.59 (d, $^2J(PC) = 7.3$ Hz, C_β), 135.75 (d, $^2J(PC) = 9.7$ Hz, C_o), 133.28 (s, C_p), 132.43 (s, C_p), 132.11 (d, $^4J(PC) = 2.3$ Hz, C_p), 132.11 (d, $^2J(PC) = 9.3$ Hz, $C_{\beta'}$), 131.21 (d, $^2J(PC) = 12.1$ Hz, C_o), 130.74 (d, $^2J(PC) = 7.7$ Hz, C_o), 128.83 (d, $^3J(PC) = 9.6$ Hz, C_m), 128.26 (d, $^3J(PC) = 10.1$ Hz, C_m), 128.15 (d, $^3J(PC) = 10.4$ Hz, C_m), 126.26 (d, $^1J(PC) = 49.0$ Hz, C_α), 123.36 (d, $^1J(PC) = 50.0$ Hz, C_α), 120.00 (d, $^3J(PC) = 9.7$ Hz, $C_{\gamma'}$), 105.56 (apparent t, $J(PC) = 2.3$ Hz, η^6-C_6Me_6), 32.91 (d, $^1J(PC) = 28.4$ Hz, CH_2), 17.52 (d, $^3J(PC) = 12.2$ Hz, CH_3), 17.20 (d, $^3J(PC) = 12.4$ Hz, CH_3), 15.40 (s, η^6-C_6Me_6).

2.2.20. [(η^6-p-$MeC_6H_4CHMe_2$)Ru(DMPP)(ADPP)Cl]PF_6 (**20**)

^1H-NMR (499.8 MHz, CD_3NO_2, 25°C) δ 7.40–7.85 (m, 15H, Ph), 6.82 (dq, $^2J(PH) = 34.0$ Hz, $^4J(HH) = 1.0$ Hz, 1H, H_α), 6.81 (dq, $^2J(PH) = 31.5$ Hz, $^4J(HH) = 1.0$ Hz, 1H, H_α), 5.61 (ddd, $^3J(HH) = 6.0$ Hz, $J(PH) = 3.5$

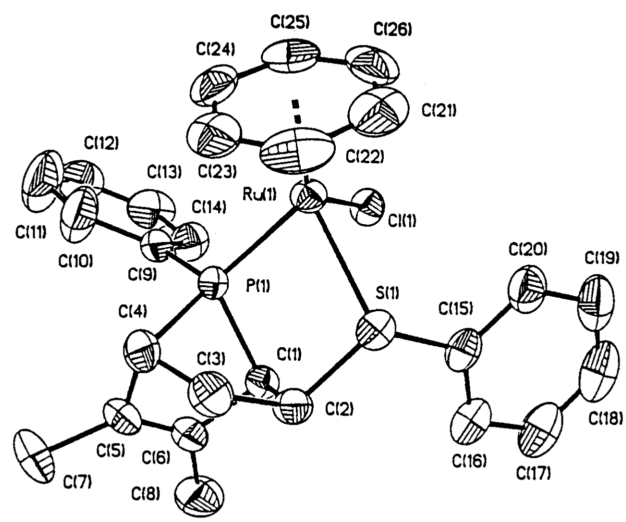

Fig. 14. Structural drawing of the cation of **14** (hydrogen atoms omitted) showing the atom numbering scheme (40% probability ellipsoids).

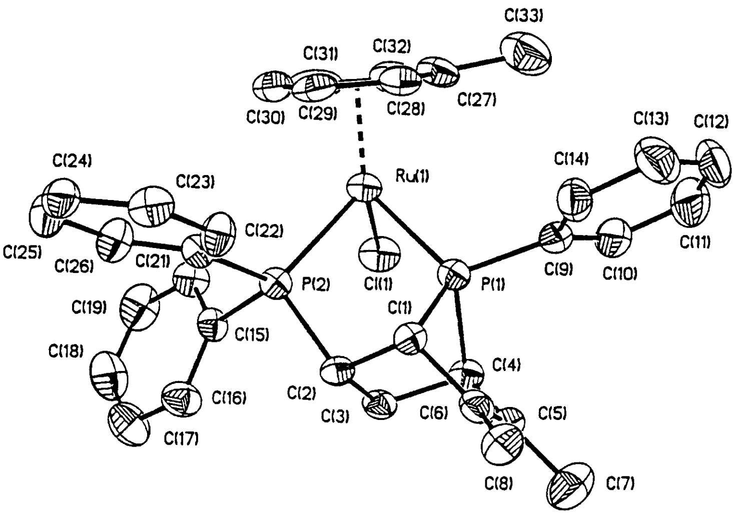

Fig. 15. Structural drawing of the cation of **16** (hydrogen atoms omitted) showing the atom numbering scheme (40% probability ellipsoids).

Hz, ^4J(HH) = 1.0 Hz, 1H, Cy), 5.39 (ddd, ^3J(HH) = 6.0 Hz, J(PH) = 3.0 Hz, ^4J(HH) = 1.0 Hz, 1H, Cy), 5.33 (ddddd, $^3J(H_aH_b)$ = 17.0 Hz, $^3J(H_aH_c)$ = 10.0 Hz, $^3J(H_aH_{\alpha'})$ = 7.5 Hz, $^3J(H_aH_{\alpha''})$ = 7.4 Hz, ^3J(PH) = 4.5 Hz, 1H, H_a), 5.20 (dd, ^3J(HH) = 6.0 Hz, ^4J(HH) = 1.0 Hz, 1H, Cy), 5.16 (dd, ^3J(HH) = 6.0 Hz, ^4J(HH) = 1.0 Hz, 1H, Cy), 4.87 (apparent ddt, $^3J(H_aH_c)$ = 10.0 Hz, $^2J(H_bH_c)$ = 1.5 Hz, $^4J(H_{\alpha'}H_c)$ = ^4J(PH) = 1.0 Hz, 1H, H_c), 4.72 (apparent dddt, $^3J(H_aH_b)$ = 17.0 Hz, $^4J(H_bH_{\alpha'})$ = $^4J(H_bH_{\alpha''})$ = 4.0 Hz, $^2J(H_bH_c)$ = ^4J(PH) = 1.0 Hz, 1H, H_b), 3.57 (ddddd, $^2J(H_{\alpha'}H_{\alpha'})$ = 15.5 Hz, ^2J(PH) = 8.0 Hz, $^3J(H_aH_{\alpha'})$ = 7.5 Hz, $^4J(H_bH_{\alpha'})$ = 4.0 Hz, $^4J(H_cH_{\alpha'})$ = 1.0 Hz, 1H, $H_{\alpha'}$), 2.62 (q, ^3J(HH) = 7.0 Hz, 1H, CH), 2.49 (apparent dt, $^2J(H_{\alpha'}H_{\alpha'})$ = 15.5 Hz, ^2J(PH) = $^3J(H_aH_{\alpha''})$ = 7.4 Hz, 1H, $H_{\alpha''}$), 2.18 (d, ^4J(HH) = 1.0 Hz, 3H, CH_3), 2.01 (d, ^4J(HH) = 1.0 Hz, 3H, CH_3), 1.90 (s, 3H, CH_3), 1.05 (d, ^3J(HH) = 7.0 Hz, 3H, CH_3), 1.05 (d, ^3J(HH) = 7.0 Hz, 3H, CH_3). $^{13}C\{^1H\}$-NMR (125.7 MHz, CD_3NO_2, 25°C) δ 154.86 (d, ^2J(PC) = 9.8 Hz, C_β), 152.43 (d, ^2J(PC) = 9.9 Hz, C_β), 134.20 (dd, ^1J(PC) = 52.5 Hz, ^2J(PC) = 2.3 Hz, C_i), 133.98 (d, ^2J(PC) = 9.6 Hz, C_o), 133.93 (dd, ^1J(PC) = 46.4 Hz, ^3J(PC) = 1.6 Hz, C_i), 132.51 (d, ^2J(PC) = 8.5 Hz, C_o), 131.70 (d, ^2J(PC) = 8.3 Hz, C_o), 131.56 (d, ^4J(PC) = 2.5 Hz, C_p), 131.03 (d, ^4J(PC) = 2.5 Hz, C_p), 130.91 (d, ^4J(PC) = 2.6 Hz, C_p), 129.86 (d, ^2J(PC) = 12.2 Hz, $C_{\beta'}$), 128.98 (dd, ^1J(PC) = 46.6 Hz, ^3J(PC) = 1.4 Hz, C_i), 128.69 (d, ^3J(PC) = 10.2 Hz, C_m), 128.57 (d, ^3J(PC) = 9.9 Hz, C_m), 128.37 (d, ^3J(PC) = 10.0 Hz, C_m), 125.52 (d, ^1J(PC) = 52.2 Hz, C_α), 124.81 (d, J(PC) = 2.1 Hz, Cy), 123.45 (d, ^1J(PC) = 50.8 Hz, C_α), 119.68 (d, ^3J(PC) = 9.8 Hz, $C_{\gamma'}$), 99.56 (s, Cy), 99.10 (dd, J(PC) = 3.7, 1.9 Hz, Cy), 95.07 (s, Cy), 92.41 (d, J(PC) = 2.8 Hz, Cy), 88.90 (d, J(PC) = 8.0 Hz, Cy), 32.07 (d, ^1J(PC) = 26.8 Hz, $C_{\alpha'}$), 30.84 (s, CH), 20.85 (s, CH_3), 20.10 (s, CH_3), 16.97 (s, CH_3), 16.56 (d, ^3J(PC) = 12.6 Hz, CH_3), 16.45 (d, ^3J(PC) = 12.9 Hz, CH_3).

2.3. *X-ray data collection and processing*

Crystals of the complexes were obtained from $ClCH_2CH_2Cl$–ether (**1**), acetone–ether (**2**, **3b**, **6**, **9**, **10**, **17**, **18**), CH_2Cl_2–ether (**4**, **14**, **20**), CH_3NO_2–ether (**3a**, **7**), CH_2Cl_2–ether (**5**, **11**), CH_3NO_2–acetone–ether (**13**) or CH_2Cl_2–CH_3OH–ether (**19**) mixtures, mounted on glass fibers coated with epoxy and placed on a Siemens P4 diffractometer. Intensity data were taken in the ω-mode at 298 K with Mo–K_α graphite monochromated radiation (λ = 0.71073 Å). Three check reflections monitored every 100 reflections showed random ($<2\%$) variation during the data collections. The data

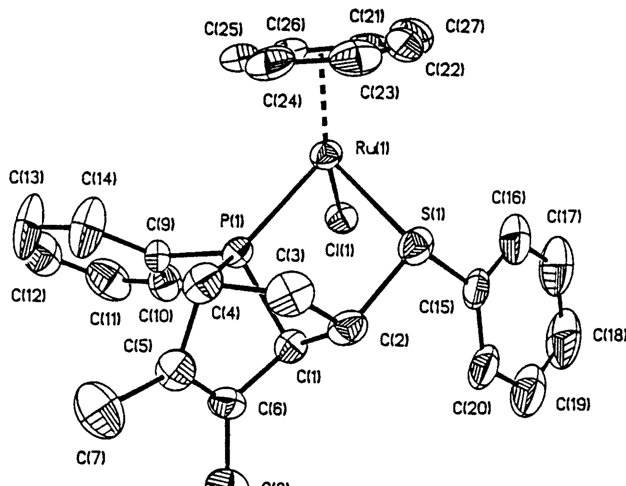

Fig. 16. Structural drawing of the cation of **17** (hydrogen atoms omitted) showing the atom numbering scheme (40% probability ellipsoids).

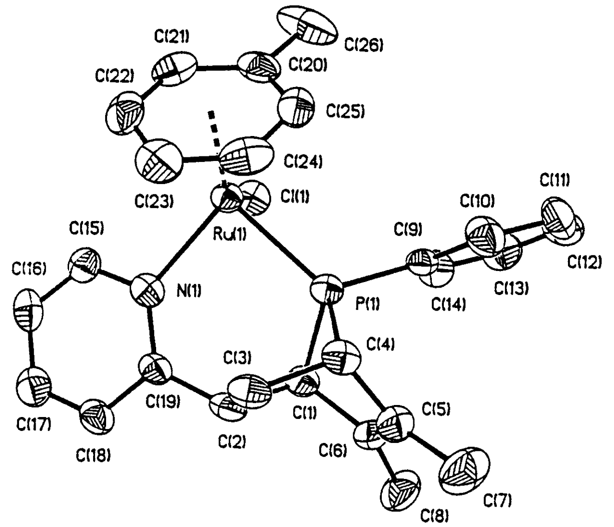

Fig. 17. Structural drawing of the cation of **18** (hydrogen atoms omitted) showing the atom numbering scheme (40% probability ellipsoids).

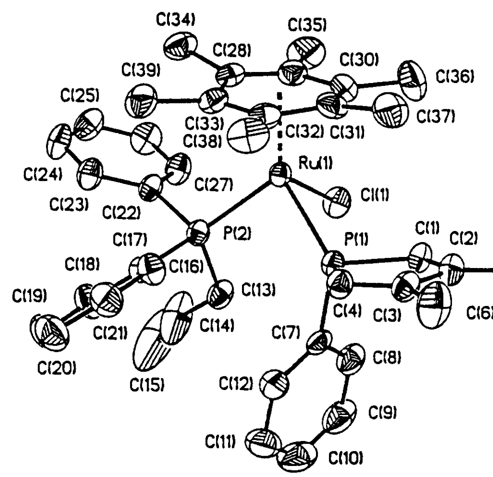

Fig. 18. Structural drawing of the cation of **19** (hydrogen atoms omitted) showing the atom numbering scheme (40% probability ellipsoids).

were corrected for Lorentz, polarization effects, and absorption using an emperical model derived from azimuthal data collections. Scattering factors and corrections for anomalous dispersions were taken from a standard source. [11] Calculations were performed with the Siemens SHELXTL PLUS version 5.10 software package on a personal computer. The structures were solved by direct (**3b**, **6**, **11**, **14**, **18**, **20**) or Patterson (**1**, **2**, **3a**, **4**, **5**, **7**, **8**, **9**, **10**, **12**, **13**, **16**, **17**, **19**) methods. Anisotropic thermal parameters were assigned to all non-hydrogen atoms. Hydrogen atoms were refined at calculated positions with a riding model in which the C–H vector was fixed at 0.96 Å. Compounds **1**, **7**, **9**, **12**, and **19** crystallized as acetone, CH_3NO_2–$ClCH_2CH_2Cl$, H_2O, acetone and CH_2Cl_2 solvates, respectively. For **7** there are two inequivalent cations in the asymmetric unit. Complex **20** spontaneously resolved. The absolute configuration was determined by refinement of the Flack parameters [12]. Crystallographic data are given in Table 3.

3. Results

The (η^6-arene)Ru(DMPP)Cl_2 complexes (DMPP = 3,4-dimethyl-1-phenylphosphole) react with $NaPF_6$ and the dieneophilic ligands L [L = $Ph_2PCH=CH_2$ (DPVP), $Me_2NC(O)CH=CH_2$ (DMAA), MeC(O)CH = CH_2 (MVK), PhSCH = CH_2 (PVS), PhS(O)CH = CH_2 (PVSO), and 2-vinylpyridine (2VP)] to form the undetected [(η^6-arene)Ru(DMPP)(L)Cl]PF_6 intermediates that undergo spontaneous intramolecular cycloaddition reactions as illustrated schematically in reaction 4. The fact that the mixed ligand intermediates could not be detected suggests that the [4 + 2] Diels–Alder cycloaddition reactions are faster than the ligand substitution reactions preceding them and the latter are rate determining. This is generally the case for these facile cycloadditions [1].

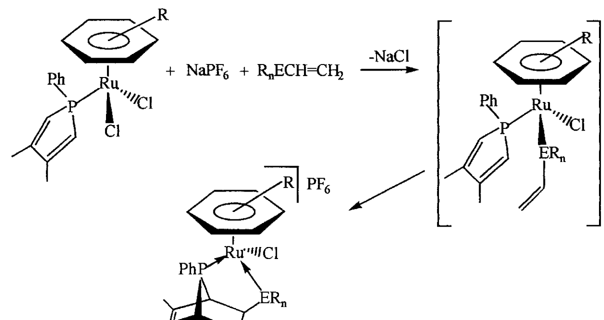

(4)

1-18

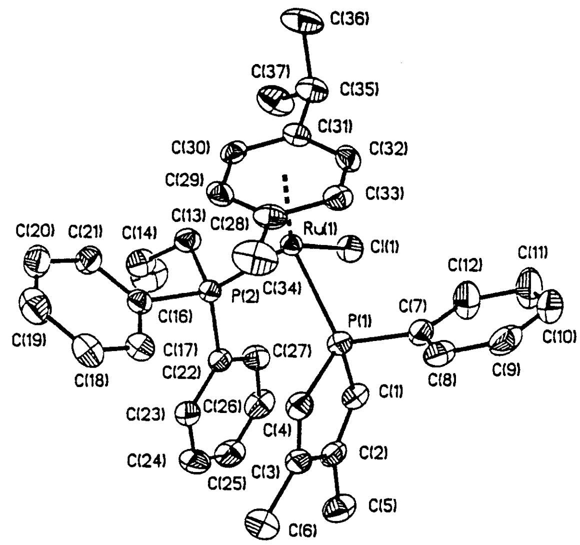

Fig. 19. Structural drawing of the cation of **20** (hydrogen atoms omitted) showing the atom numbering scheme (40% probability ellipsoids).

Table 5
^{1}H Chemical shifts (ppm) for the norbornene ring protons of compounds **1**–**18**

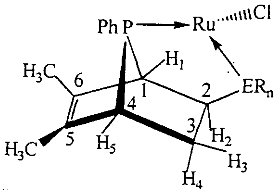

Compound	Diastereomer	H_1	H_2	H_3	H_4	H_5	$CH_3(5)$	$CH_3(6)$	Arene	Dieneophile
(1)	B	3.97	3.33	2.27	1.53	3.06	1.83	1.36	HMB	DPVP
(2)	A	3.48	4.04	1.68	2.31	3.75	1.80	1.56	HMB	PVS
(3a)	B	3.95	4.07	2.11	1.40	3.10	1.86	1.38	HMB	PVSO
(3b)	A	3.26	4.50	2.76	2.29	3.84	1.86	1.59	HMB	PVSO
(4)	A	3.14	3.40	2.02	2.19	4.06	1.85	1.46	HMB	MVK
(5)	A	3.19	3.27	2.03	1.95	3.92	1.86	1.46	HMB	DMAA
(6)	A	2.65	3.43	2.24	2.36	4.00	1.88	1.45	HMB	2VP
(7)	B	3.87	3.56	2.40	1.67	3.19	1.71	1.49	Cy	DPVP
(8a)	B	3.56	4.10	1.93	2.48	3.71	1.68	1.66	Cy	PVS
(8b)	A	3.34	2.53	2.53	1.82	3.24	1.77	1.51	Cy	PVS
(9)	B	4.04	4.30	2.15	1.56	3.23	1.88	1.52	Cy	PVSO
(10)	A	3.17	3.57	2.42	2.20	4.26	1.71	1.53	Cy	MVK
(11)	A	2.97	3.20	2.13	1.84	3.91	1.50	1.32	Cy	DMAA
(12)	A	2.84	3.51	2.50	2.38	4.01	1.75	1.56	Cy	2VP
(13)	B	3.93	3.53	2.41	1.73	3.27	1.88	1.54	Bz	DPVP
(14)	A	3.56	4.08	2.03	2.39	3.71	1.69	1.63	Bz	PVS
(15)	A	2.86	3.50	2.60	2.35	4.00	1.74	1.60	Bz	2VP
(16)	B	3.92	3.51	2.45	1.72	3.26	1.88	1.53	Tol	DPVP
(17)	A	3.56	4.08	2.02	2.37	3.71	1.69	1.68	Tol	PVS
(18)	A	2.86	3.50	2.57	2.34	3.97	1.75	1.59	Tol	2VP

The [(η^6-arene)Ru(DMPP)(DPVP)Cl]PF_6 Diels–Alder adducts were also prepared by reaction 5.

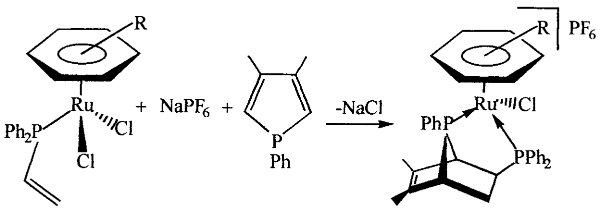

The diastereomeric ratios of the common products of reactions 4 and 5, as determined by $^{31}P\{^1H\}$-NMR spectroscopy of the crude products, were the same suggesting that the diastereo-meric ratios are under thermodynamic control. Moreover, interconversion of the diastereomers does not occur.

No Diels–Alder cycloadducts were formed in the reaction of (η^6-MeC_6H_5)Ru(DMPP)Cl_2 or (η^6-C_6H_6)Ru(DMPP)Cl_2 with $NaPF_6$ and PVSO, MVK, or DMAA. The reactions of (η^6-C_6Me_6) Ru(DMPP)Cl_2 and (η^6-*p*-$MeC_6H_4CHMe_2$)Ru(DMPP)Cl_2 with $NaPF_6$ and allyldiphenylphosphine (ADPP) produced the mixed ligand complexes [(η^6-arene)Ru(DMPP)-(ADPP)Cl]PF_6 which did not undergo subsequent Diels–Alder cycloadditions even after heating at 84°C in $ClCH_2CH_2Cl$ solutions for 1 week. This contrasts with our previous report [1d] of Diels–Alder adduct formation upon reaction of [(Cp)Ru(DMPP)$_2$-(CH_3CN)]PF_6 with diallylphenylphosphine.

The Diels–Alder reactions described herein provide ready syntheses of chiral complexes containing conformationally rigid bidentate ligands with diastereoselectivities that are generally quite high and are a function of the magnitudes of intraligand steric effects.

New compounds were characterized by ^1H-, $^{13}C\{^1H\}$-, and $^{31}P\{^1H\}$-NMR spectroscopy. Proton and carbon chemical shift assignments were made by detailed analysis of $^1H/^1H$ decoupling, $^1H\{^{31}P\}$, APT, and $^1H/^{13}C$ HETCOR experiments and are given in the experimental section. The proton resonance line shapes were similar to those that we have described [13] for Ru(CO)Cl_2_ (DMPP) complexes of some of these ligands. The NMR spectral data are characteristic of the assigned structures.

4. Discussion

4.1. Diastereoselectivity

Because these [4 + 2] Diels–Alder cycloadditions all occur intramolecularly [1] within the ruthenium coordination sphere to form the *syn*-*exo*-7-phosphanorbornene skeleton (illustrated below) the absolute configuration of the C(1) and C(4) stereocenters are fixed and only those at C(2) (the ring conjunction carbon), E, and P(7) may vary.

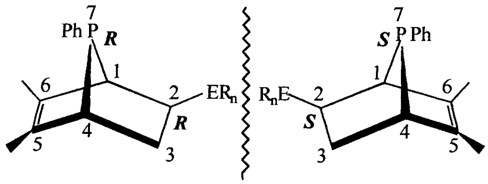

For the cases where ER$_n$ is –PPh$_2$, –S(O)Ph or –SPh, in both enantiomers of these ligands the stereochemistry of C(2) is the same as that of P(7). When ER$_n$ is –C(O)NMe$_2$, –C(O)CH$_3$, or -2- pyridyl the stereochemistry of C(2) is opposite that of P(7) as a result of different priorities in the CIP sequence rules [14] even though the relative positions of the ER$_n$ moieties remain the same. Thus, for ease of discussion, we will refer to the absolute configuration of these chiral ligands by a single descriptor, R or S. Ruthenium becomes a stereocenter in the products and may have either R or S absolute configuration leading to two racemic diastereomers (R_LS_{Ru}–S_LR_{Ru}) and (S_LS_{Ru}–R_LR_{Ru}) for all products except those derived from PVS and PVSO as illustrated below.

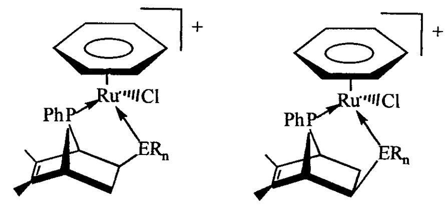

(R_LS_{Ru} / S_LR_{Ru}) (A) (S_LS_{Ru} / R_LR_{Ru}) (B)

In the sulfide and sulfoxide complexes, sulfur becomes a stereocenter such that for these complexes up to four racemic diastereomers, namely ($R_LS_SS_{Ru}$–$S_LR_SR_{Ru}$), ($R_LS_SS_{Ru}$–$S_LR_SR_{Ru}$), ($S_LS_SS_{Ru}$–$R_LR_SR_{Ru}$), and ($S_LR_SS_{Ru}$–$R_LS_SR_{Ru}$) may be formed.

For simplicity, we will call the enantiomeric pairs of diastereomers A and B, respectively and will consider the stereochemistry at sulfur separately. The geometric structures of the major diastereomers of most of these products were determined by X-ray crystallography (Figs. 1–19). These structures consist of isolated cations and anions with no short interionic contacts. Selected bond distances and angles are given in Table 4. As can be seen in Figs. 1, 7, 13 and 16, the major diastereomer of each of the [(η^6-arene)Ru– (DMPP)(DPVP)Cl]PF$_6$ complexes is diastereomer B. For each of these complexes

Table 6
$^{13}C\{^1H\}$ chemical shifts (ppm) for the norbornene ring carbons of compounds **1**–**18**

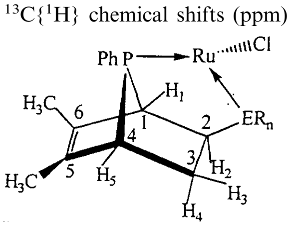

Compound	Diastereomer	C_1	C_2	C_3	C_4	C_5	C_6	$CH_3(5)$	$CH_3(6)$	Dieneophile
(1)	B	58.05	34.27	31.17	50.12	140.20	130.72	12.24	13.97	DPVP
(2)	A	57.68	42.36	32.54	45.53	130.48	129.61	12.98	13.41	PVS
(3a)	B	52.07	65.28	28.31	48.51	140.76	140.64	12.63	13.93	PVSO
(3b)	A	53.79	60.87	27.80	44.74	141.57	139.44	12.78	13.57	PVSO
(4)	A	49.22	49.35	30.54	47.41	138.89	134.67	12.54	13.14	MVK
(5)	A	53.30	39.78	29.29	46.45	139.11	135.49	12.56	13.14	DMAA
(6)	A	49.07	46.82	31.18	47.18	136.66	135.03	12.55	13.10	2VP
(7)	B	57.13	31.26	30.45	48.73	139.05	131.00	12.33	13.89	DPVP
(8a)	B	55.95	40.97	33.20	48.11	130.10	128.85	13.00	13.51	PVS
(8b)	A	56.13	43.88	33.05	45.87	130.53	130.06	12.72	13.76	PVS
(9)	B	52.73	63.35	28.66	46.87	140.42	140.17	12.74	13.90	PVSO
(10)	A	48.15	49.53	32.10	50.91	140.46	135.13	14.11	14.52	MVK
(11)	A	51.91	39.92	30.81	50.16	140.53	136.03	14.21	14.58	DMAA
(12)	A	47.44	45.90	31.91	50.10	137.75	134.34	12.82	13.13	2VP
(13)	B	57.44	31.08	30.23	47.65	138.95	131.34	12.37	13.89	DPVP
(14)	A	55.51	40.64	33.27	48.74	140.77	129.92	12.92	13.47	PVS
(15)	A	47.38	45.84	30.02	51.07	137.52	134.40	12.74	13.03	2VP
(16)	B	57.44	31.19	30.35	47.89	138.97	131.21	12.39	13.88	DPVP
(17)	A	55.79	40.76	33.27	48.49	140.75	129.88	12.94	13.49	PVS
(18)	A	47.54	45.93	32.07	50.71	137.50	134.35	12.73	13.03	2VP

Table 7
Redox characteristics of the complexes [a]

Compound	Complex formula	Ru(II)/Ru(III) $E_{1/2}$ V (ΔE, mV)	Reference
	$(\eta^6\text{-}C_6Me_6)Ru(DMPP)Cl_2$	0.43 (125)	[1f]
	$(\eta^6\text{-}p\text{-}MeC_6H_4CHMe_2)Ru(DMPP)Cl_2$	0.64 (120)	[1f]
	$(\eta^6\text{-}MeC_6H_5)Ru(DMPP)Cl_2$	0.69 (88)	[1f]
	$(\eta^6\text{-}C_6H_6)Ru(DMPP)Cl_2$	0.75 (71)	[1f]
	$[(Cp)Ru(DMPP)_2(DPVP)]PF_6$ [4+2] A	0.78 [b]	[1d]
	$[(Cp)Ru(DMPP)_2(DPVP)]PF_6$ [4+2] B	0.83 [b]	[1d]
	$[(Cp)Ru(DMPP)_2(PVSO)]PF_6$ [4+2]	0.96 [b]	[1d]
	$[(Cp)Ru(DMPP)_2(PVS)]PF_6$ [4+2]	0.63 (95)	[1d]
	$[(Cp)Ru(DMPP)_2(2VP)]PF_6$ [4+2]	0.52 (53)	[1d]
(1)	$[(\eta^6\text{-}C_6Me_6)Ru(DMPP)(DPVP)Cl]PF_6$ [4+2]	0.94 (101)	This work
(2)	$[(\eta^6\text{-}C_6Me_6)Ru(DMPP)(PVS)Cl]PF_6$ [4+2]	0.95 (240)	This work
(3)	$[(\eta^6\text{-}C_6Me_6)Ru(DMPP)(PVSO)Cl]PF_6$ [4+2]	1.20 (256)	This work
(4)	$[(\eta^6\text{-}C_6Me_6)Ru(DMPP)(MVK)Cl]PF_6$ [4+2]	1.11 [b]	This work
(5)	$[(\eta^6\text{-}C_6Me_6)Ru(DMPP)(DMAA)Cl]PF_6$ [4+2]	0.84 (208)	This work
(6)	$[(\eta^6\text{-}C_6Me_6)Ru(DMPP)(2VP)Cl]PF_6$ [4+2]	1.03 (136)	This work
(7)	$[(\eta^6\text{-}p\text{-}MeC_6H_4CHMe_2)Ru(DMPP)(DPVP)Cl]PF_6$ [4+2]	1.09 (122)	This work
(8)	$[(\eta^6\text{-}p\text{-}MeC_6H_4CHMe_2)Ru(DMPP)(PVS)Cl]PF_6$ [4+2]	1.14 (195)	This work
(9)	$[(\eta^6\text{-}p\text{-}MeC_6H_4CHMe_2)Ru(DMPP)(PVSO)Cl]PF_6$ [4+2]	1.40 (220)	This work
(10)	$[(\eta^6\text{-}p\text{-}MeC_6H_4CHMe_2)Ru(DMPP)(MVK)Cl]PF_6$ [4+2]	0.71 [b]	This work
(11)	$[(\eta^6\text{-}p\text{-}MeC_6H_4CHMe_2)Ru(DMPP)(DMAA)Cl]PF_6$ [4+2]	0.98 (163)	This work
(12)	$[(\eta^6\text{-}p\text{-}MeC_6H_4CHMe_2)Ru(DMPP)(2VP)Cl]PF_6$ [4+2]	1.10 (216)	This work
(13)	$[(\eta^6\text{-}C_6H_6)Ru(DMPP)(DPVP)Cl]PF_6$ [4+2]	1.15 (166)	This work
(14)	$[(\eta^6\text{-}C_6H_6)Ru(DMPP)(PVS)Cl]PF_6$ [4+2]	1.24 (112)	This work
(15)	$[(\eta^6\text{-}C_6H_6)Ru(DMPP)(2VP)Cl]PF_6$ [4+2]	1.24 [b]	This work
(16)	$[(\eta^6\text{-}MeC_6H_5)Ru(DMPP)(DPVP)Cl]PF_6$ [4+2]	1.14 [b]	This work
(17)	$[(\eta^6\text{-}MeC_6H_5)Ru(DMPP)(PVS)Cl]PF_6$ [4+2]	1.30 [b]	This work
(18)	$[(\eta^6\text{-}MeC_6H_5)Ru(DMPP)(2VP)Cl]PF_6$ [4+2]	1.16 (191)	This work
(19)	$[(\eta^6\text{-}C_6Me_6)Ru(DMPP)(ADPP)Cl]PF_6$ [4+2]	1.06 (123)	This work
(20)	$[(\eta^6\text{-}p\text{-}MeC_6H_4CHMe_2)Ru(DMPP)(ADPP)Cl]PF_6$ [4+2]	1.20 (147)	This work

[a] In CH_2Cl_2 containing 0.1 M TBAP at 25°C, $v = 250$ mV s^{-1}. E values are vs. F_c^+/F_c. Cp = $\eta^5\text{-}C_5H_5$.
[b] E_{pa} only.

the Ru–P_1 distance (2.294 Å), ave.) is slightly shorter than the Ru–P_2 distance (2.327 Å, ave.). Comparing the Ru–P_1 distances in **1** with **19** and **7** with **20** we note that upon chelate ring formation the Ru–P_1 bond distance shortens slightly as expected. If these complexes were ideally octahedral, the sum of the P_1–Ru–P_2, P_1–Ru–Cl, and P_2– Ru–Cl angles would be 270°. These angle sums increase in the sequence: $\eta^6\text{-}C_6Me_6$ (256.27°) < $\eta^6\text{-}p\text{-}MeC_6H_4CHMe_2$ (257.71°) < $\eta^6\text{-}MeC_6H_5$ (259.54°) ≅ $\eta^6\text{-}C_6H_6$ (259.42°) in concert with the steric bulk of the arene decreasing in the same order. Another measure of the steric interaction between the arene and the substituents on the 7-phosphanorbornene ring is the dihedral angle between the arene and P_1P_2Cl planes. These dihedral angles decrease in the sequence: $\eta^6\text{-}C_6Me_6$ (5.6°) > $\eta^6\text{-}p\text{-}MeC_6H_4CHMe_2$ (2.9°) > $\eta^6\text{-}C_6H_6$ (0.5°) ≅ $\eta^6\text{-}MeC_6H_5$ (0.2°). The percent diastereomeric excesses (%DE = %major diastereomer − %minor diastereomer), determined by $^{31}P\{^1H\}$-NMR spectroscopy of the crude products (Table 2) fall in the order: $\eta^6\text{-}C_6H_6$ (> 99%) > $\eta^6\text{-}p\text{-}MeC_6H_4CHMe_2$ (87.8%) ≅ $\eta^6\text{-}MeC_6H_5$ (86%) > $\eta^6\text{-}C_6Me_6$ (82%) suggesting that the% DE decreases roughly as the steric bulk of the arene increases. For the analogous reactions of the η^5-Cp complexes (reactions 1–3) the % DEs were much lower (15.4, 58.4, and 0%, respectively) and in reactions 1 and 2 the major diastereomer is A. From these results it appears that diastereomer A should in general be the thermodynamically favored diastereomer unless the steric interactions between the η^6-arene and the PPh_2 group on the 2-position of the norbornene ring become quite large, in which case diastereomer B will be favored. For the products of the reactions involving PVSO (**3a**, **3b**, and **9**) and compounds **8a** and **8b** (L = PVS) diastereomer B was the major diastereomer formed. For all other products diastereomer A was formed exclusively at the limit of detection by $^{31}P\{^1H\}$-NMR spectroscopy. Compound **3a** forms as the racemic diastereomers ($S_LS_SS_{Ru}$–$R_LR_SR_{Ru}$), **3b** as the racemic diastereomers ($S_LR_SS_{Ru}$–$R_LS_SR_{Ru}$), and **9** as the racemic diastereomers ($S_LS_SS_{Ru}$–$R_LR_SR_{Ru}$).

4.2. Spectral characterization

We have previously noted [15] that when two diastereomers of the DMPP/DPVP Diels–Alder cycloadducts are formed that diastereomer A may be distinguished from diastereomer B by $^{31}P\{^{1}H\}$-NMR spectroscopy. In general the chemical shift difference of the phosphorus resonances, $\Delta\delta = \delta P_7 - \delta P_2$ is greater for diastereomer A than for diastereomer B. As the data in Table 2 show, except for **1a** and **1b**, where these differences are essentially the same, this criterion still holds. For all other complexes, when two diastereomers were observed, the $^{31}P\{^{1}H\}$ chemical shift for diastereomer A occurs downfield of that for diastereomer B.

The ^{1}H and ^{13}C chemical shifts of the 7-phosphanorbornene ring nuclei are also diagnostic of the nature of the diastereomer formed. For convenience of discussion these data are collected in Tables 5 and 6, respectively. As can be seen in Fig. 3 protons 1, 3, 4, and 5 and all the ring carbons are in considerably different environments for the two diastereomers. Considering compounds **3a** and **3b**, which are diastereomers B and A, respectively, we note that the chemical shifts of protons 1–5 for diastereomers A all occur downfield of the corresponding resonances for diastereomer B. Comparing the data for compounds **3** with **9** and **2**, **8** and **14** with **17**, and **4** with **10**, and **5** with **11**, and **6**, **12**, and **15** with **18** we note that the nature of the diastereomer has a greater influence on these chemical shifts than does either the nature of the arene or the 2-substituent. The relative chemical shifts of protons 1 and 5 are particularly diagnostic. Except for the four PVS adducts (**2**, **8**, **14**, and **17**) the chemical shifts of proton-1 are downfield of those of proton-5 for diastereomer B and the converse is true for diastereomer A. Similar relationships are observed for the relative chemical shifts of the methyl proton [$CH_3(5)$ and $CH_3(6)$] resonances. These chemical shift differences most likely arise because of the location of these nuclei in either the shielding or deshielding regions of the magnetically anisotropic arene rings. Similar arguments apply to the relative ^{13}C chemical shifts of the norbornene ring carbons (C_1 and C_4, C_5 and C_6) and the two methyl carbons (Table 6). The PVS adducts undergo epimerization at sulfur on the NMR time scale [1d], as evidenced by broad resonances for some of the phenyl carbons in their $^{13}C\{^{1}H\}$-NMR spectra. This dynamic process has an effect on these relative chemical shifts. With this body of data, X-ray crystallography and multinuclear NMR spectroscopy, it is now possible to identify the diastereomer by multinuclear NMR spectroscopy.

The infrared spectra of all these complexes exhibit ν(PF) vibrations at 838 and 557 cm^{-1} as expected for PF_6^- salts. The spectra of the DMAA and PVSO adducts exhibit ν(CO) and ν(SO) near 1590 and 1080 cm^{-1}, respectively supporting sulfur and oxygen coordination, respectively [16], for these potentially ambidentate ligands, as found in the crystal structures. The spectra of the MVK adducts exhibit ν(CO) near 1700 cm^{-1} as compared to that of the free ligand (1717 cm^{-1}) supporting oxygen coordination as in the crystal structures.

4.3. Redox properties of the complexes

The electron-donor abilities of coordinated ligands and the complex geometry affect the redox properties of ruthenium complexes. [17] The electrochemical behavior of the complexes prepared in this study was investigated by cyclic voltammetry (Table 7). For all complexes the Ru(II)–Ru(III) redox couple is a quasi-reversible one-electron process or a process that approaches reversiblity. For **1**, **2**, **3**, **5**, **6**, **7**, **8**, **9**, **11**, **12**, **13**, **18**, **19**, and **20**, the follow-up chemical step is slow and reversible voltammograms were observed. For the other complexes, the follow-up chemical step is fast as no cathodic wave could be seen on the return sweep, even at high scan rates. The data in Table 7 are very similar to those reported [13] for Ru(DMPP) (CO)Cl_2 complexes of some of these ligands. The Ru(II)–Ru(III) potentials ranged from 0.56 to 1.15 V for the carbonyl complexes. The $E_{1/2}$ values depend principally upon the σ-donor and/or π-acceptor abilities of the ligands. Comparison of the $E_{1/2}$ values of the η^5-C_5H_5 and η^6-arene complexes shows that oxidation of the η^5-C_5H_5 complexes occurs at lower potentials than for analogous η^6-arene complexes. Among the η^6-arene complexes the ease of oxidation generally decreases in the sequence η^6-$C_6Me_6 > \eta^6$-*p*-$MeC_6H_4CHMe_2 > \eta^6$-$MeC_6H_5 \cong \eta^6$-C_6H_6. Thus, the donor abilities of these ligands toward Ru(II) decreases in the order η^5-$C_5H_5 > \eta^6$-$C_6Me_6 > \eta^6$-*p*-$MeC_6H_4CHMe_2 > \eta^6$-Me-$C_6H_5 \cong \eta^6$-C_6H_6. The σ-donor abilities of the 2-substituted-7- phosphanorbornenes are generally in the order $P \sim S > N \sim O$ as determined from the comparative $E_{1/2}$ values. Comparing the $E_{1/2}$ values of **1** with **19** and **7** with **20** shows that chelate ring formation increases the donor ability slightly.

4.4. Conclusions

The [(η^6-arene)Ru(DMPP)Cl_2] complexes undergo intramolecular [4 + 2] Diels–Alder cycloaddition reactions with a greater variety of dieneophiles than any previously investigated complexes. In general, the diastereoselectivities of these reactions are quite high. It is lowest with the sulfur donors PVS and PVSO and this may be related to the fact that sulfur also becomes a stereocenter in the products derived from these two dieneophiles. The diastereoselectivity of these Diels–Alder cycloaddition reactions is under thermodynamic control. The most favored diastereomer is formed such as to minimize intramolecular steric interactions. These new [(η^6-arene)Ru(AB)Cl]PF_6 complexes are currently being tested as catalysts for transfer hydrogenation of ketones, alkenes and imines.

5. Supplementary material

Tables of X-ray data in CIF format for compounds **1**, **2**, **3a**, **3b**, **4**, **5**, **6**, **7**, **8**, **9**, **10**, **11**, **12**, **13**, **14**, **16**, **17**, **18**, **19** and **20** have been deposited with the Cambridge Crystallographic Data Centre, CCDC nos. 144240–144259. Copies of this information may be obtained free of charge from The Director, CCDC, 12 Union Road, Cambridge, CB2 1EZ, UK (Fax: +44-1223-336033; e-mail: deposit@ccdc.cam.ac.uk or www: http://www.ccdc.cam.ac.uk).

Acknowledgements

This research was supported by an award from the Research Corporation for which we are grateful. We are also grateful to the National Science Foundation (Grant no. CHE-9214294) for funds to purchase the 500 MHz NMR spectrometer.

References

[1] (a) Lj. Solujić, E.B. Milosavljević, J.H. Nelson, N.W. Alcock, J. Fischer, Inorg. Chem. 28 (1989) 3453. (b) S. Affandi, J.H. Nelson, J. Fischer, Inorg. Chem. 28 (1989) 4536. (c) D. Bhaduri, J.H. Nelson, C.L. Day, R.A. Jacobson, Lj. Solujić, E.B. Milosavljević, Organometallics 11 (1992) 4069. (d) H.-L. Ji, J.H. Nelson, A. De Cian, J. Fischer, Lj. Solujić, E.B. Milosavljević, Organometallics 11 (1992) 1840. (e) J.H. Nelson, in: L.D. Quin, J.G. Verkade, (Eds.), Phosphorus-31-NMR Spectral Properties in Compound Characterization and Structural Analysis, VCH, Deerfield Beach, FL, 1994, pp. 203–214. (f) K.D. Redwine, V.J. Catalano, J.H. Nelson, Syn. React. Inorg. Met. Org. Chem. 29 (1999) 395.

[2] K. Maitra, V.J. Catalano, J.H. Nelson, J. Am. Chem. Soc. 119 (1997) 12 560.

[3] (a) P.-H. Leung, S.K. Loh, K.F. Mok, A.J.P. White, D.J. Williams, J. Chem. Soc. Chem. Commun. (1996) 591. (b) B.H. Aw, P.-H. Leung, A.J.P. White, D.J. Williams, Organometallics 15 (1996) 3640. (c) S. Selvaratnam, K.F. Mok, P.-H. Leung, A.J.P. White, D.J. Williams, Inorg. Chem. 35 (1996) 4798. (d) P.-H. Leung, S.K. Loh, K.F. Mok, A.J.P. White, D.J. Williams, J. Chem. Soc. Dalton Trans. (1996) 4443. (e) B.H. Aw, T.S.A. Hor, S. Selvaratnam, A.J.P. White, D.J. Williams, N.H. Rees, W. McFarlane, P.-H. Leung, Inorg. Chem. 36 (1997) 2138. (f) P.-H. Leung, S. Selvaratnam, C.R. Cheng, K.F. Mok, N.H. Rees, W. McFarlane, J. Chem. Soc. Chem. Commun. (1997) 751. (g) A.M. Liu, K.F. Mok, P.-H. Leung, J. Chem. Soc. Chem. Commun. (1997) 2397. (h) P.-H. Leung, S.Y. Siah, A.J.P. White, D.J. Williams, J. Chem. Soc. Dalton Trans. (1998) 893. (i) Y. Song, J.J. Vittal, S.-H. Chan, P.-H. Leung, Organometallics 18 (1999) 650. (j) P.-H. Leung, G. He, H. Lang, A. Liu, S.K. Loh, S. Selvaratnam, K.F. Mok, A.J.P. White, D.J. Williams, Tetrahedron 56 (2000) 7.

[4] N. Gül, J.H. Nelson, Tetrahedron 56 (2000) 71.

[5] F. Mathey, F. Mercier, Tetrahedron Lett. 22 (1981) 319.

[6] (a) K. Mashima, K. Kusano, T. Ohta, R. Noyori, H. Takahya, J. Chem. Soc. Chem. Commun. (1989) 1208. (b) K. Püntener, L. Schwink, P. Knochel, Tetrahedron Lett. 37 (1996) 8165.

[7] T. Ohta, T. Miyake, H. Takaya, J. Chem. Soc. Chem. Commun. (1992) 1725.

[8] N. Uematsu, A. Fujii, S. Hashiguchi, T. Ikariya, R. Noyori, J. Am. Chem. Soc. 36 (1996) 288.

[9] A. Breque, F. Mathey, P. Savignac, Synthesis, (1981) 983.

[10] K.D. Redwine, H.D. Hansen, S. Bowley, J. Isbell, M. Sanchez, D. Vodak, J.H. Nelson, Syn. React. Inorg. Met. Org. Chem. 30 (3) (2000) 379.

[11] International Tables for X-ray Crystallography, vol. C, D. Reidell Publishing Co. Boston, 1992.

[12] H.D. Flack, Acta Crystallogr. Sect A 39 (1983) 876.

[13] R. Vac, J.H. Nelson, E.B. Milosavljević, Lj. Solujić, J. Fischer, Inorg. Chem. 28 (1989) 4132.

[14] Absolute configurations are assigned according to the Baird–Sloan modification of the Cahn-Ingold-Prelog priority rules. See: K. Stanley, M.C. Baird, J. Am. Chem. Soc. 97 (1975) 6598 and T.E. Sloan, Top. Stereochem. 12 (1981) 1.

[15] J.H. Nelson, Coord. Chem. Rev. 139 (1995) 245.

[16] B.R. James, E. Ochaiai, J. Rempel, Inorg. Nucl. Chem. Lett. 7 (1971) 781.

[17] (a) A.B.P. Lever, Inorg. Chem. 29 (1990) 1271. (b) C.M. Duff, G.A. Heath, Inorg. Chem. 30 (1991) 2528.